



301 Mission St
Perimeter Pile
Upgrade

Calculations

Analyses for
Future Settlement

301 Mission Street
San Francisco, CA

15 November 2021

SGH Project 147041.10

SIMPSON GUMPERTZ & HEGER



Engineering of Structures
and Building Enclosures

PREPARED FOR:

Millennium Tower Association
301 Mission Street
Level B-1
San Francisco, CA 94103

PREPARED BY:

Simpson Gumpertz & Heger Inc.
1999 Harrison Street, 24th Floor
Oakland, CA 94111
Tel: 415.495.3700
Fax: 415.495.3550

TABLE OF CONTENTS

1.	BACKGROUND	2
2.	ANALYTICAL MODEL: PERFORM 3D	4
2.1	Added vertical settlements	4
2.2	Foundation lateral response modification	6
2.3	Mat Deformed Shape under settlement load	7
2.4	Substructure Analysis Results	8
2.4.1	Gravity Loads	8
2.4.2	Seismic Loads	9
2.5	Superstructure Analysis Results	14
2.5.1	Shear Wall Concrete Compressive Strains	15
2.5.2	Shear Wall Steel Tensile Strains	16
2.5.3	Composite Coupling Beam Inelastic Rotations	17
2.5.4	Shear Wall Forces	18
2.5.5	Moment Frame Column Plastic Rotations	39
2.5.6	Moment Frame and Core Coupling Beam Plastic Rotations	40
2.5.7	Outrigger Coupling Beam Rotations	41
2.5.8	North-South Direction Seismic Transient Interstory Drift Ratios	42
2.5.9	East-West Direction Interstory Drift Ratios	43
2.5.10	North-South Direction Seismic Residual Interstory Drift Ratios	44
2.5.11	East-West Direction Seismic Residual Interstory Drift Ratios	45

1. BACKGROUND

In early May 2021, the general contractor for the Perimeter Pile Upgrade (PPU), Shimmick, initiated production pile installation. As a first step in this process, Shimmick installed 36 in. casings along Fremont Street, starting at the south end, near the driveway and proceeding northward. We subsequently noted an increase in the building settlement rate along Fremont Street, resulting in some increased tilting to the west. In late June 2021, Shimmick completed installing 36 in. casings along Fremont Street. Over a two-week period, they repositioned their equipment to the Mission Street side of the building and mobilized equipment onto Fremont Street to install the deeper 24 in. piles to rock. At this time, the northwest corner of the building had settled approximately 1/2 in. since the initiation of pile installation. During the two-week period when Shimmick relocated equipment on site, the building returned to pre-construction rates of settlement, or a rate of about 1/8 in. per year.

In early July, Shimmick began installing 36 in. casings along Mission Street, and simultaneously, 24 in. piles along Fremont Street through the previously installed 36 in. casings, again working from south to north. As this work progressed, we again noted an increase in the rate of settlement and tilting to the west together with tilting to the north. On 30 July, we recommended a moratorium on 36 in. casing installation along Mission Street. Shimmick continued to install 24 in. piles along Fremont, so that we could determine the effect on building settlement of the pile installation alone. Tilting of the building to the north reduced significantly (i.e., to about pre-construction levels) with the moratorium on 36 in. casing installation but tilting of the building to the west continued with the installation of 24 in. piles along Fremont. On 24 August, we recommended a moratorium on 24 in. pile placement to allow us to determine a best course forward. At that time, the building had settled approximately 1 in. at the northwest corner since the initiation of piling activity. With the institution of the second moratorium, settlement rates again returned to pre-construction levels, where they have remained. At that time, thirty-three of the 36 in. casings and six of the 24 in. piles had been installed.

In October we initiated a pilot program to test the effectiveness of improved casing and pile installation procedures in minimizing future construction-related building settlement and tilting. Shimmick successfully completed the pilot test of a 36 in casing installation on 12-13 October. Installation of that casing and two subsequent ones demonstrates that using the improved procedures, each 36 in. casing produces about 1/50 in. settlement at the mat's centroid, and 1/16

in. at the northwest corner, resulting in approximately 0.1 in. additional tilt of the roof to the north, and approximately 3/16 in. tilt to the west per casing. This is within the range we anticipated prior to the test. The data from these installations, along with that from planned pilot installations of 24 in piles will allow the design team to estimate the maximum anticipated settlement that is likely to occur during construction of the project.

We conducted the analyses presented in this report to determine a structurally safe level of acceptable additional building settlement and tilt that will not compromise the ability of the existing building to resist a major earthquake. We conclude that the building can withstand tilt to the west of approximately 79 inches and tilt to the north of approximately 33 inches and remain structurally safe even when subjected to Maximum Considered Earthquake shaking as defined in ASCE 7-16.

2. ANALYTICAL MODEL: PERFORM 3D

For detailed descriptions of the elements in our Perform-3d model refer to calculation volumes 2 and 3 from the project permit submittal. We increased the amount of tilt by introducing additional settlement to the vertical pile springs and modified the foundation lateral response nonlinear backbone for the effects of the added pile head rotations resulting from the added tilt. The subsections below describe these modifications in detail.

2.1 Added vertical settlements

Figure 2-1 shows measured building tilt from the 20 October 2021 survey monitoring report by Slate Geotechnical Consultants (Slate). Figure 2-2 shows the building tilt as modeled in our analyses of the existing building conditions. This model is used for comparison of analyses results as a reference point in quantifying the effects of added tilt.

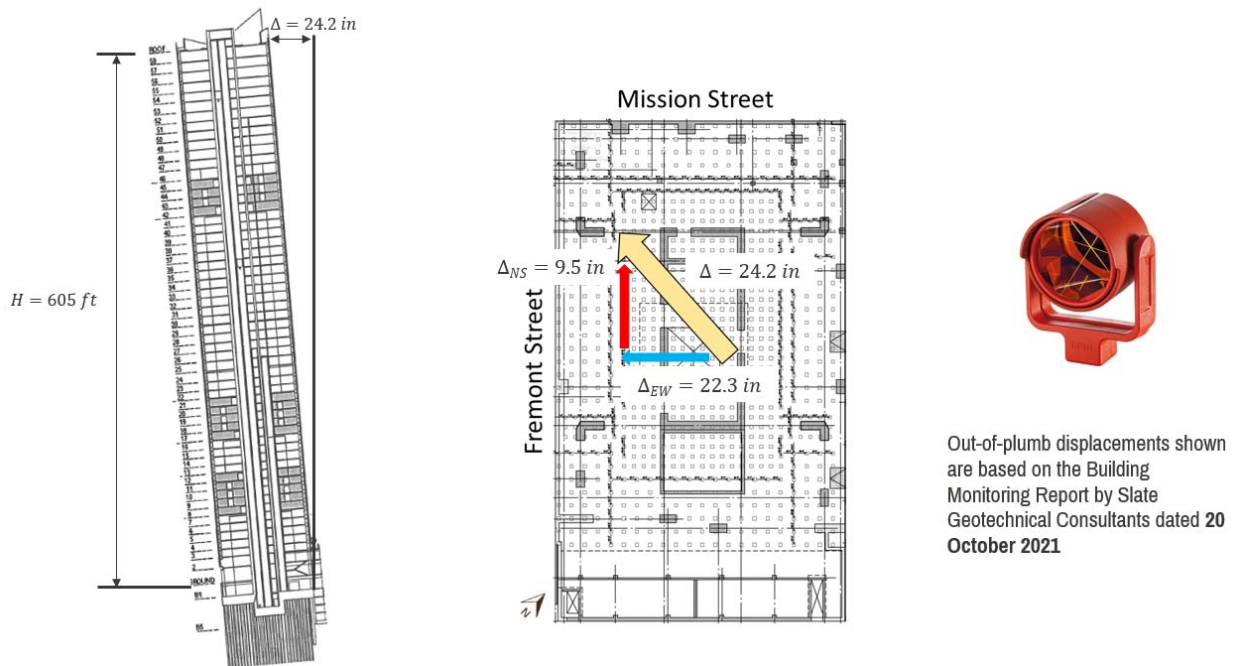


Figure 2-1 – Measured building tilt

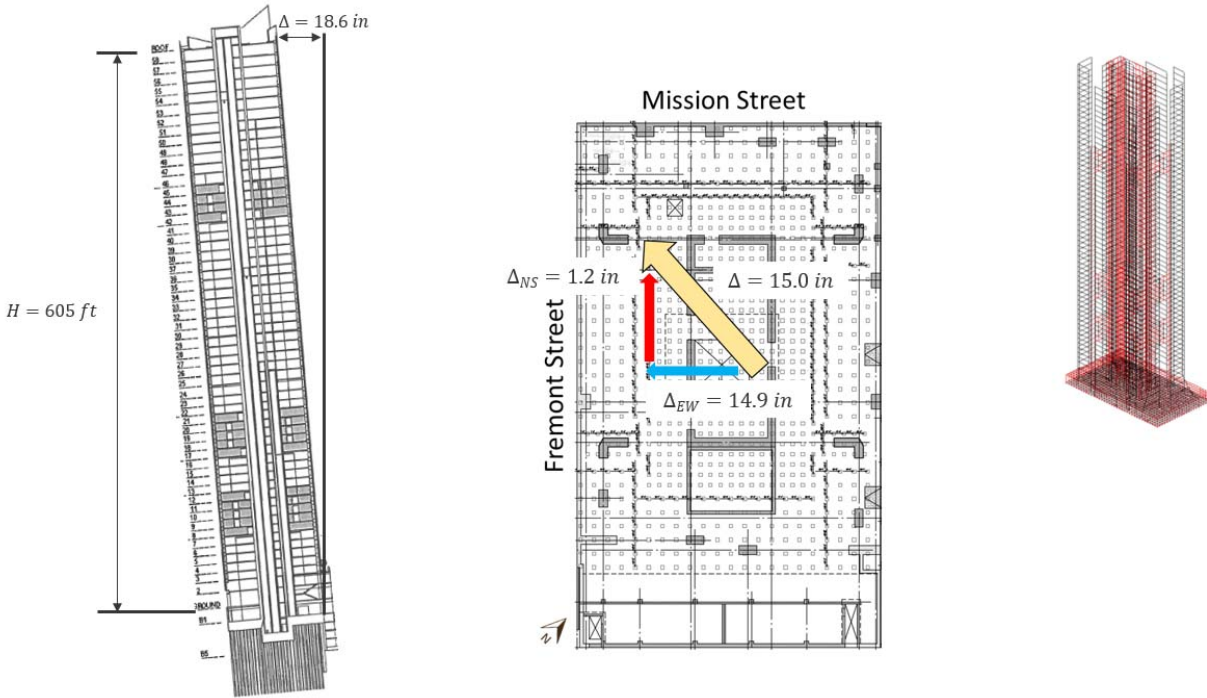


Figure 2-2 – Building tilt in Existing Conditions model

Figure 2-3 illustrates our approach to assigning additional settlement to the pile springs by modifying temperature loads and assuming the building rotates about the mat survey high point, SM-3.

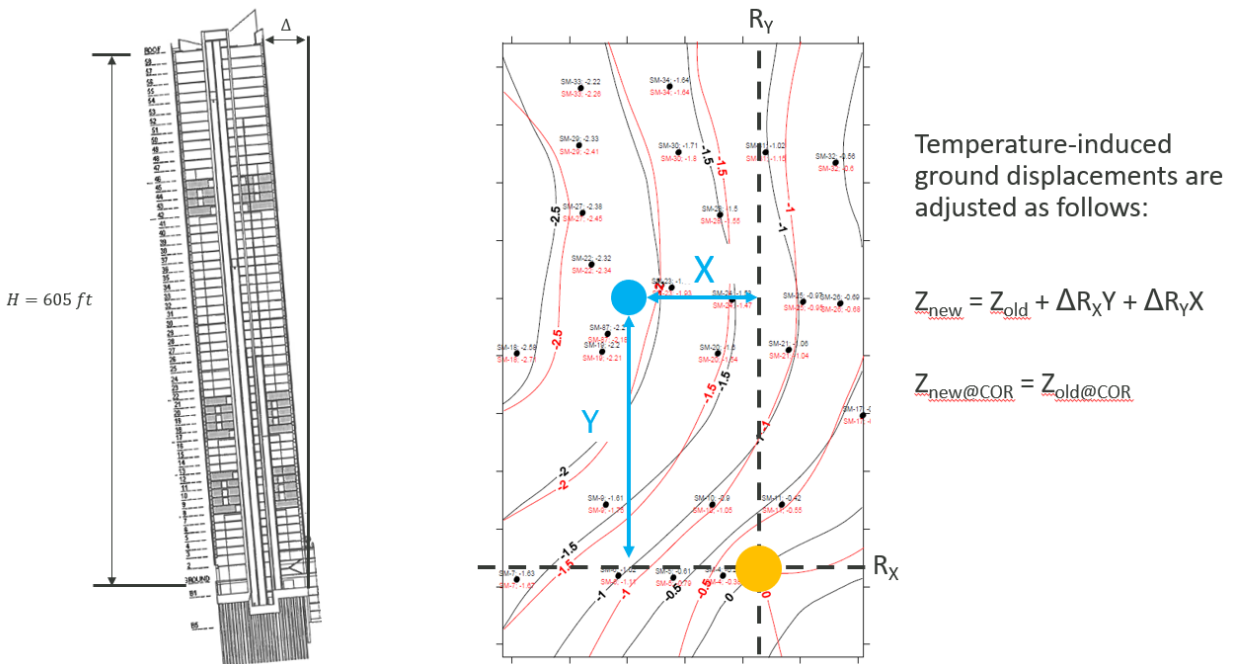


Figure 2-3 – Building tilt in Existing Conditions model

Table 2-1 shows a comparison of the east-west and north-south tilt values between the survey and the existing and maximum tilt models. The total northwest tilt in the maximum tilt model amounts to approximately 3.5 times the current building tilt.

Table 2-1 – Comparison of tilt values between the survey and the existing and maximum tilt models

Load Case	Displacement, inches		Roof Drift	
	East-West	North-South	East-West	North-South
20 October 2021	22.3	9.5	0.31%	0.13%
Existing Conditions Model	14.9	1.2	0.21%	0.02%
3.5x Current Tilt Model	79.1	32.8	1.09%	0.45%

2.2 Foundation lateral response modification

Figure 2-4 shows the lateral load effects of tilt on the building mat foundation. Tilt of the mat causes rotation in the pile heads which causes a lateral displacement in the pile similar to that of a cantilevered beam with an end moment.

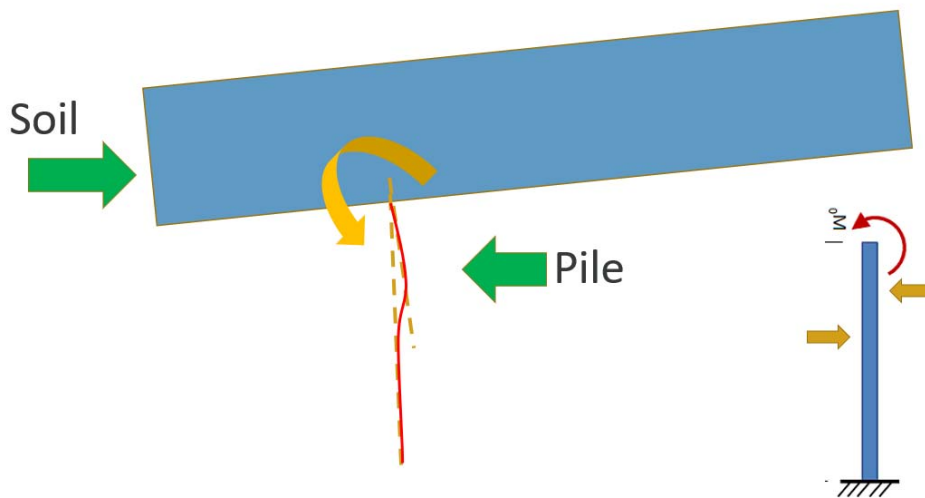


Figure 2-4 – Lateral load effects of tilt

In our permit model we accounted for the effect of pile head rotations by assigning a static load to the mat representing the sum of the lateral forces induced in the piles. In our current model, we separated the foundation pile spring from the passive soil pressure spring and assigned a displacement load to the foundation pile spring equal to the lateral displacement which results in

equilibrium of the piles. This is a more precise approach to modeling this effect than used in our prior analyses of tilt effects. Figure 2-5 conceptually illustrates the assignment of displacement preload to the model. Similarly to our original model, we applied the at-rest soil pressures as static loads to the mat.

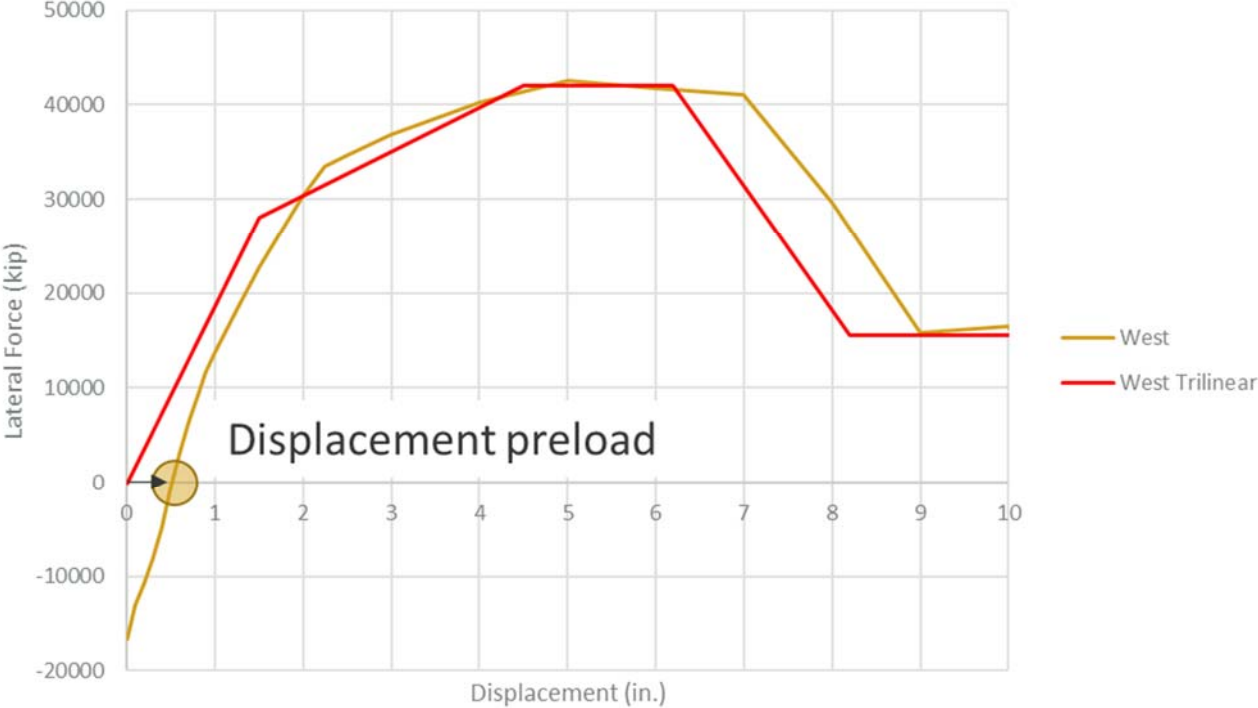


Figure 2-5 – Pile backbone displacement preload

In addition to the above changes we recomputed the lateral response backbone of the existing piles for the 3.5 times the current tilt load case and assigned it to our model. Figure 2-10 and Figure 2-11 show the cumulative lateral resistance backbones in the north-south and east-west directions, respectively.

2.3 Mat Deformed Shape under settlement load

Figure 2-6 presents a comparison of the deformed shapes of the existing conditions model and the 3.5 times the current tilt model.

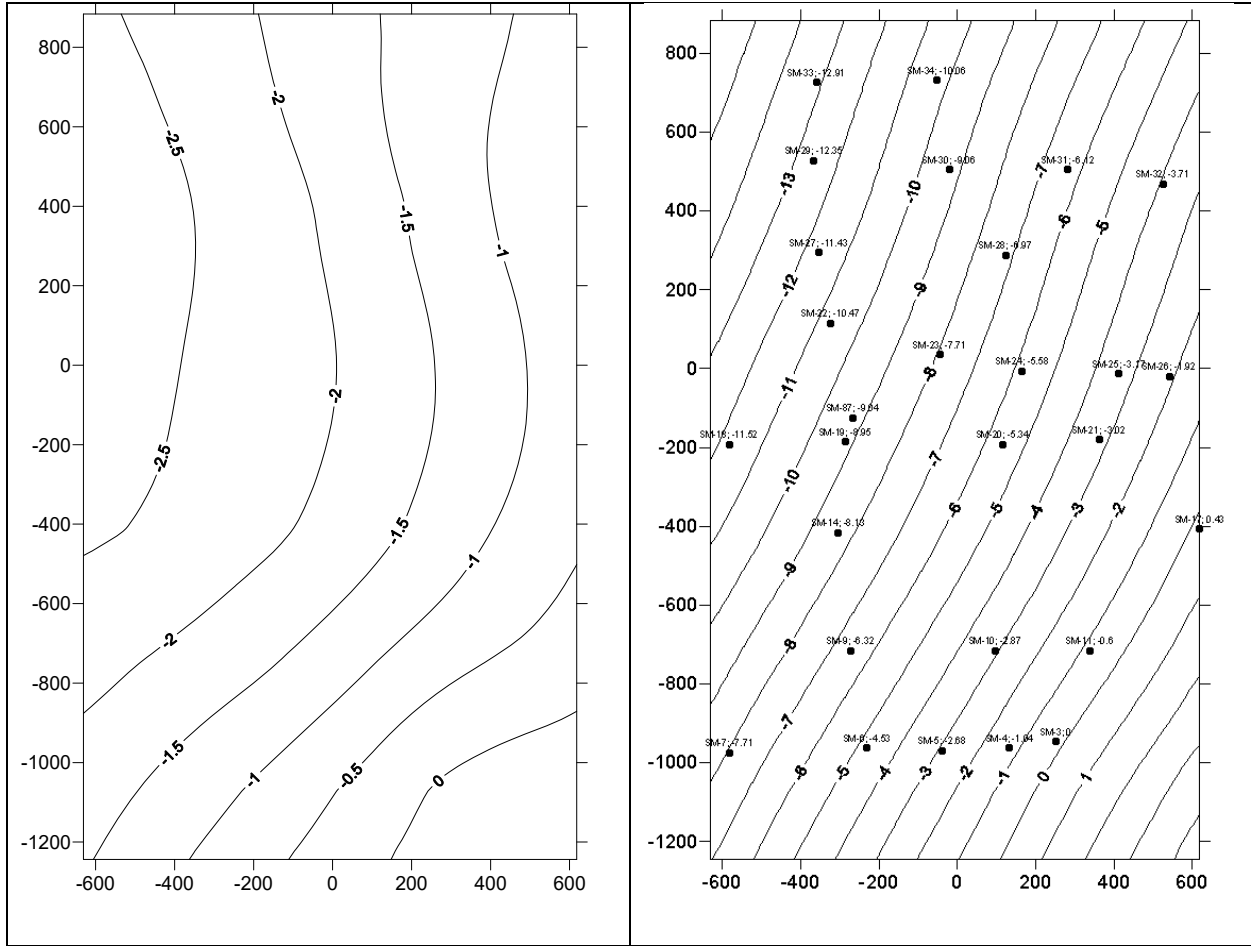


Figure 2-6 – Comparison of the mat deformed shape between the existing conditions model (left) and the 3.5x current tilt model (right)

2.4 Substructure Analysis Results

2.4.1 Gravity Loads

We checked the flexural behavior of the mat under gravity loads using the updated model of the existing conditions and 3.5 times the current tilt. Figure 2-7 shows plastic hinge rotations of the mat grillage elements relative to 1%. Green lines identify the grillage elements where minor yielding has occurred. The additional tilt has virtually no impact on the distribution of yielding under gravity load.

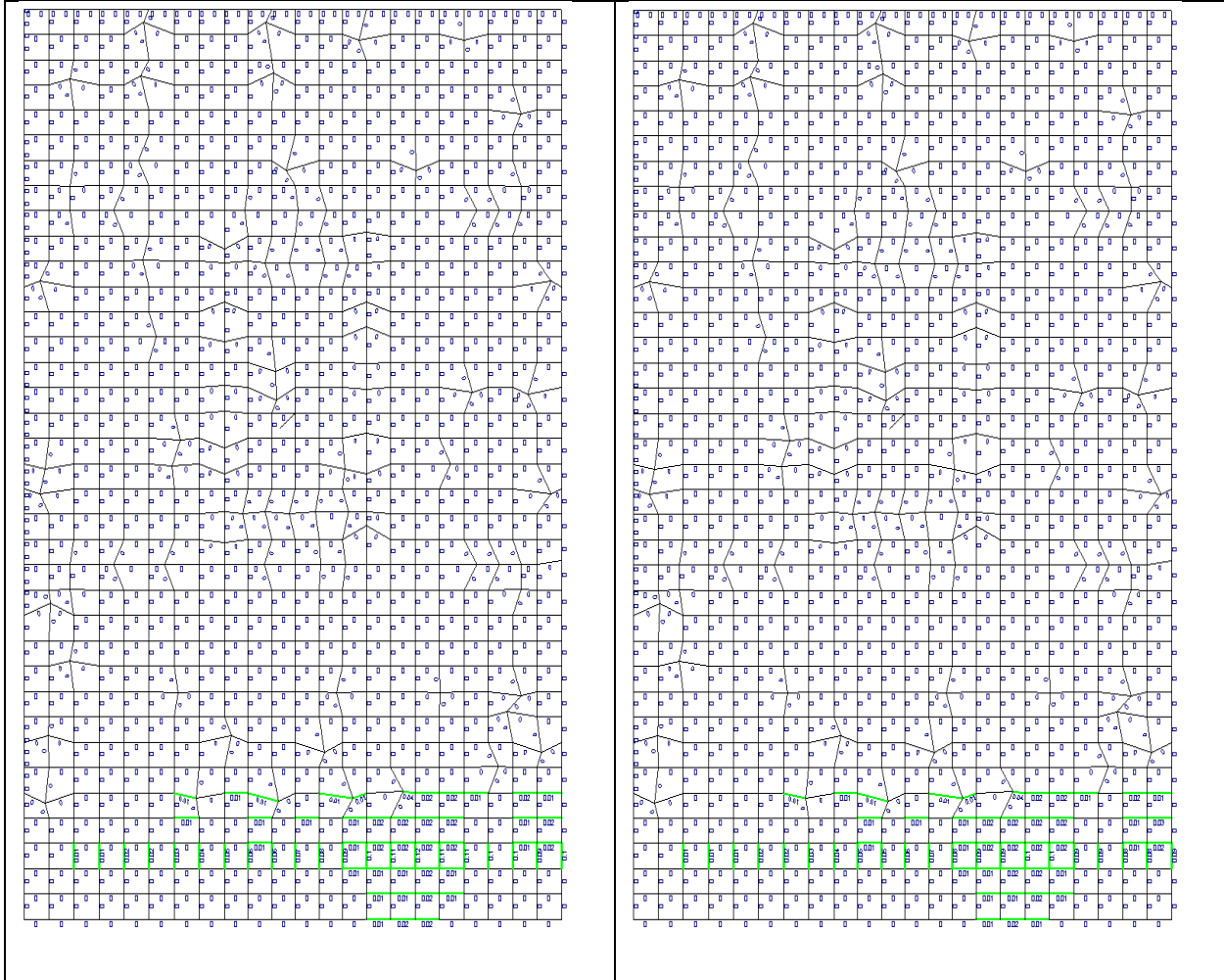


Figure 2-7 – Mat grillage inelastic rotations after jacking in percent units; existing conditions model (left) and the 3.5x current tilt model (right)

2.4.2 Seismic Loads

Figure 2-8 compares the mat shear DCRs from the existing conditions model and 3.5 times the current tilt model under dead, live, and MCE seismic response. DCR values shown in parentheses are from the existing conditions model.

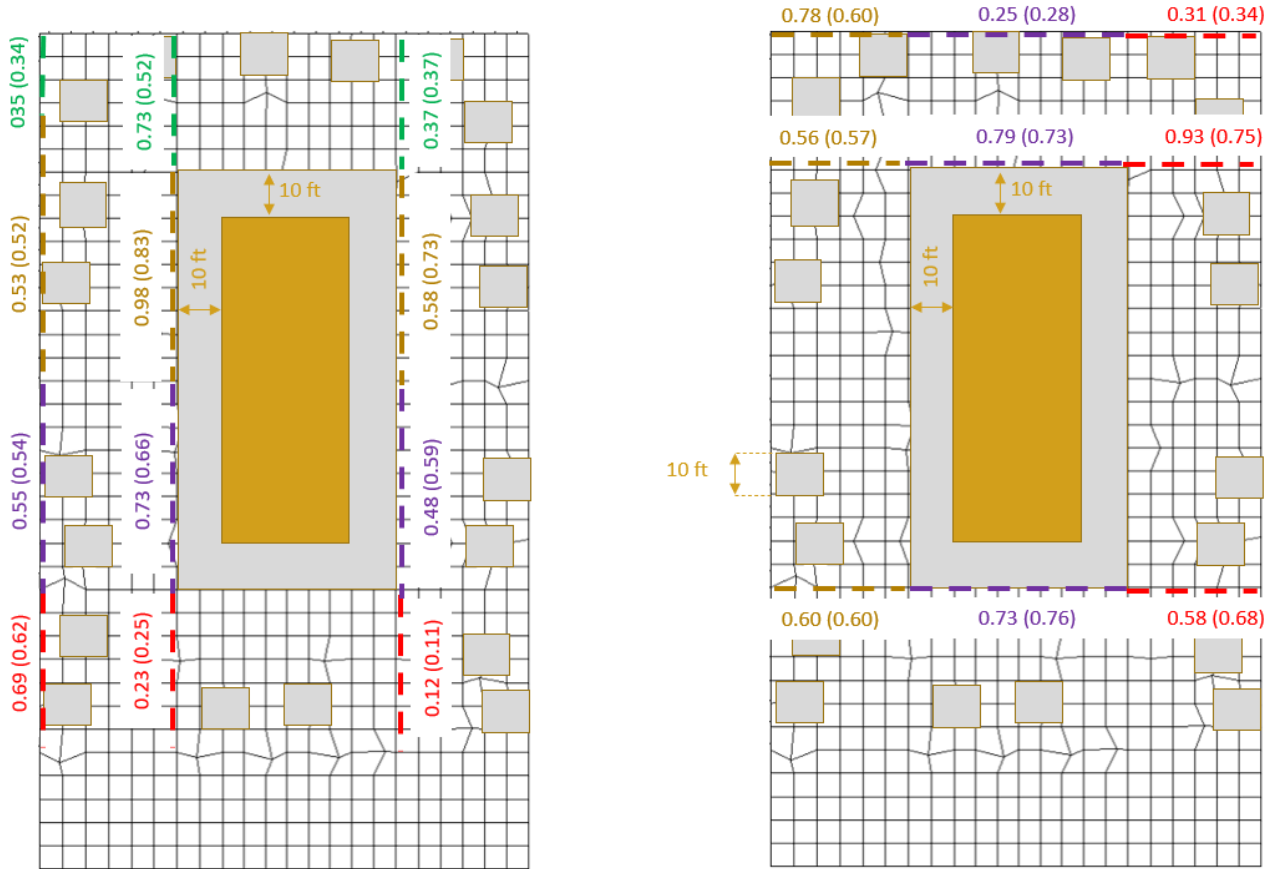


Figure 2-8 – Mat Shear DCRs

Figure 2-9 compares the dead, live, and seismic plastic hinge rotations of the mat grillage elements as a fraction of 1%.

Table 2-2, Figure 2-10, and Figure 2-11 show base displacements in the east-west and north-south directions. We observe an increase in lateral displacement at the base of the tower of quarter to half an inch relative to that in the existing condition model. This is a result of the increased lateral force exerted by the piles on the tower as a result of the additional tilt. Please note that the realistic increase in displacement is likely less than that computed our analyses due to the fact that we simulated pile lateral response using short-term soil springs that do not account for the long-term effects of creep and relaxation in the soils.

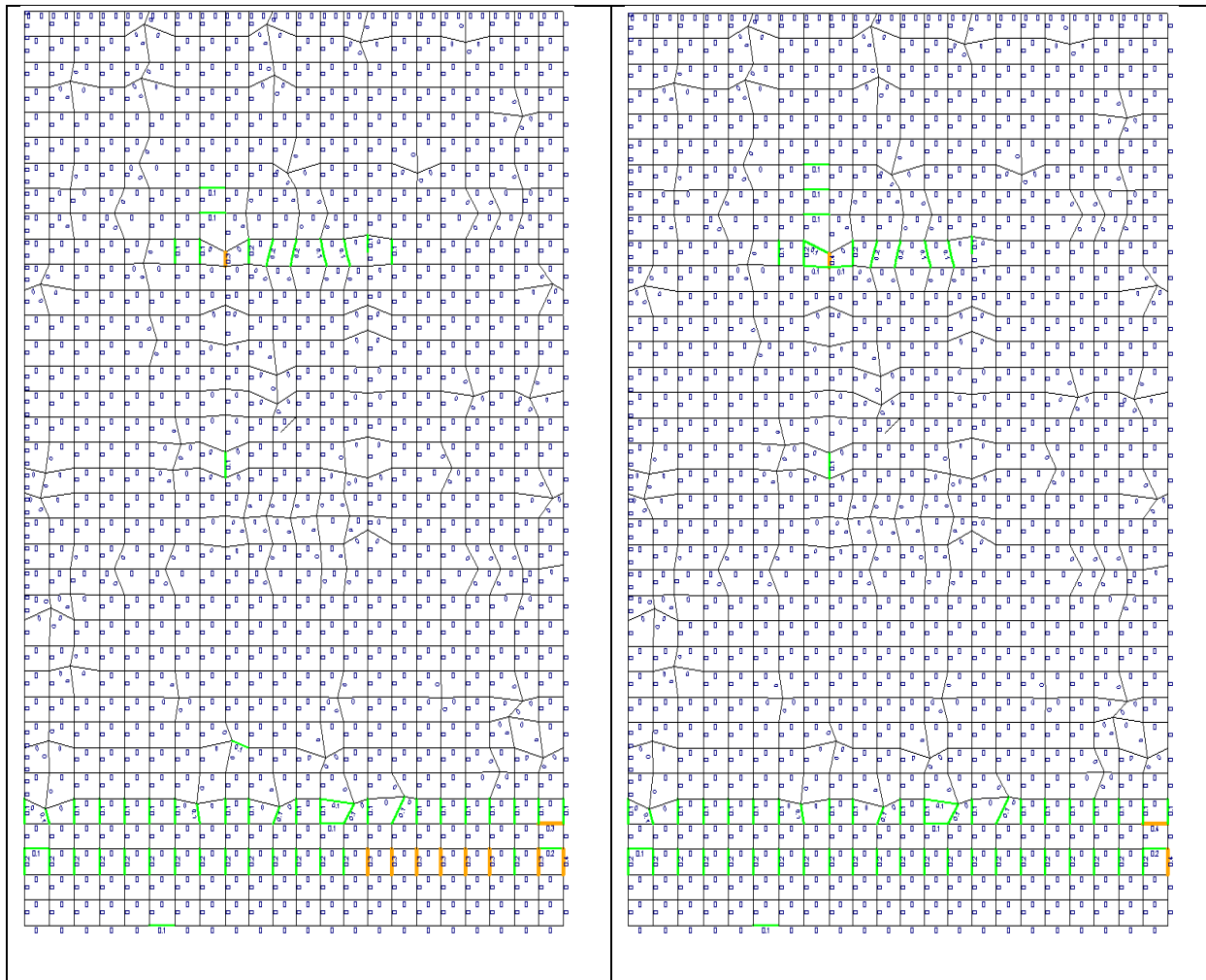


Figure 2-9 – Mat grillage seismic inelastic rotations in percent units (Average of 11 Ground Motions); permit model (left), updated model (right)

Table 2-2: Maximum Tower Foundation Displacements due to MCE

Ground Motion Record	Existing Conditions				3.5 x Current Tilt			
	East	West	North	South	East	West	North	South
RSN__36 Borrego	0.6	0.6	0.7	1.5	0.5	1.4	0.9	1.7
RSN_900 Landers	0.6	0.6	0.4	3.2	0.6	1.3	0.4	3.4
RSN1155 Kocaeli	1.4	0.9	0.6	0.8	1.3	1.6	0.8	1.2
RSN1177 Kocaeli	0.5	0.9	0.9	1.9	0.5	1.6	0.9	2.0
RSN1244 ChiChi	0.5	0.6	2.0	1.5	0.7	1.1	1.9	1.7
RSN1476 ChiChi	0.8	0.6	0.6	1.1	0.7	1.4	0.7	1.6
RSN2107 Denali Carlo	1.2	0.7	0.5	1.0	1.1	1.5	0.4	1.4
RSN2111 Denali	1.1	0.8	1.4	1.2	1.2	1.8	1.4	1.3
RSN5829 Sierra Mex	1.2	0.5	0.4	1.7	1.3	1.1	0.6	1.9
RSN5832 Sierra Mex	0.6	0.8	0.6	1.0	0.9	1.4	0.7	1.3
RSN6887 Darfield	0.4	0.6	2.3	2.8	0.3	1.3	2.0	3.4
Average of 11 Ground Motions	0.8	0.7	0.9	1.6	0.8	1.4	1.0	1.9

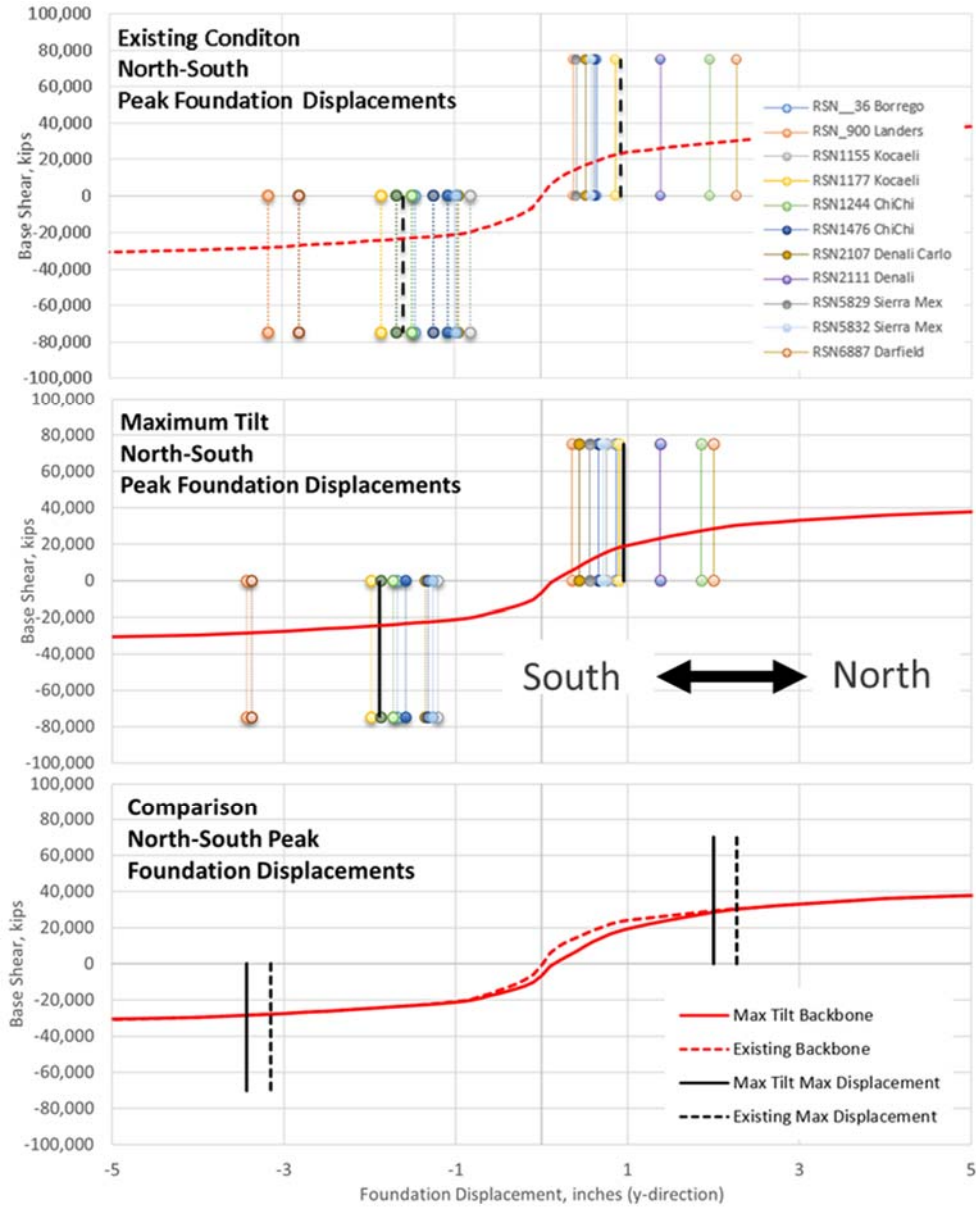


Figure 2-10 – North-South Peak Tower Foundation Displacements due to the MCE

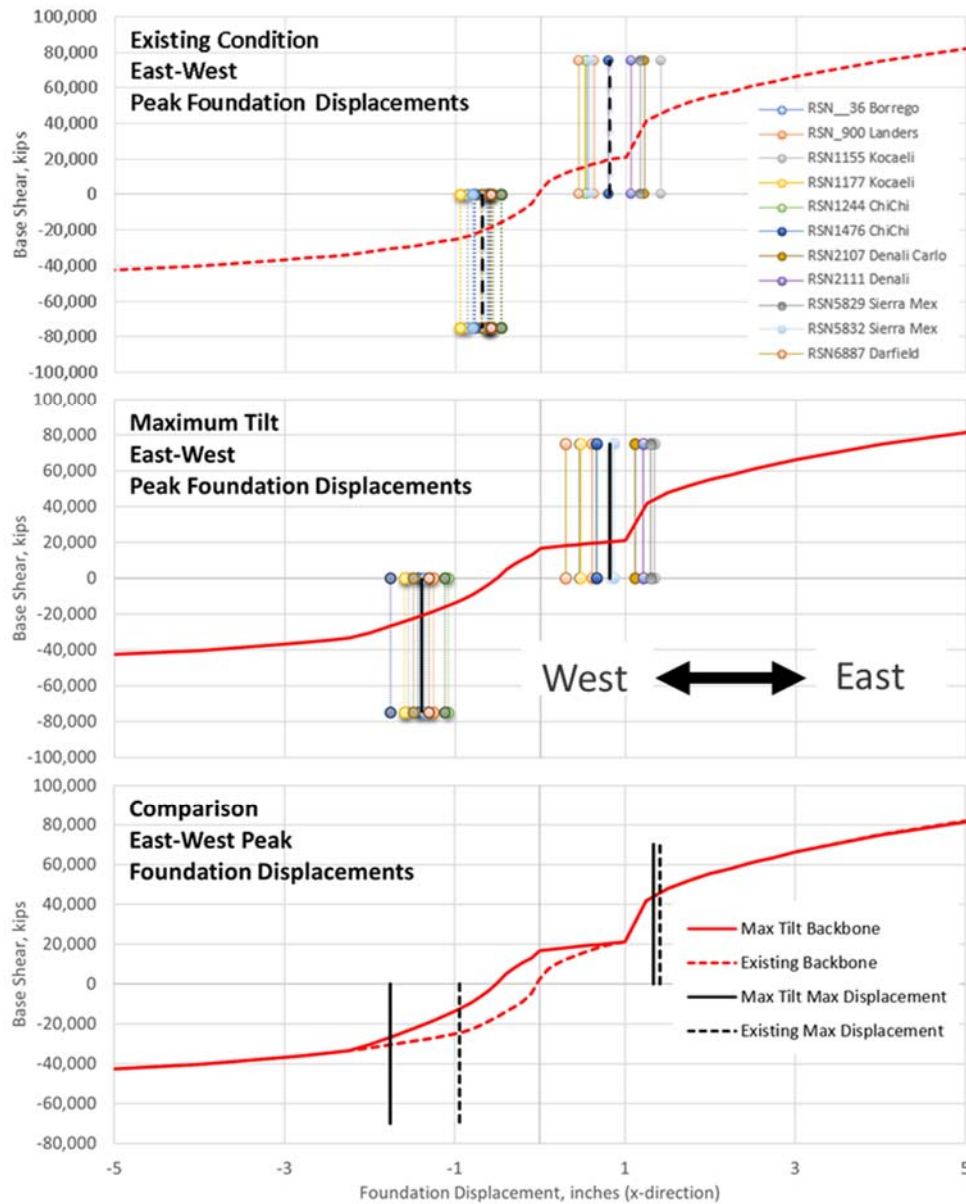
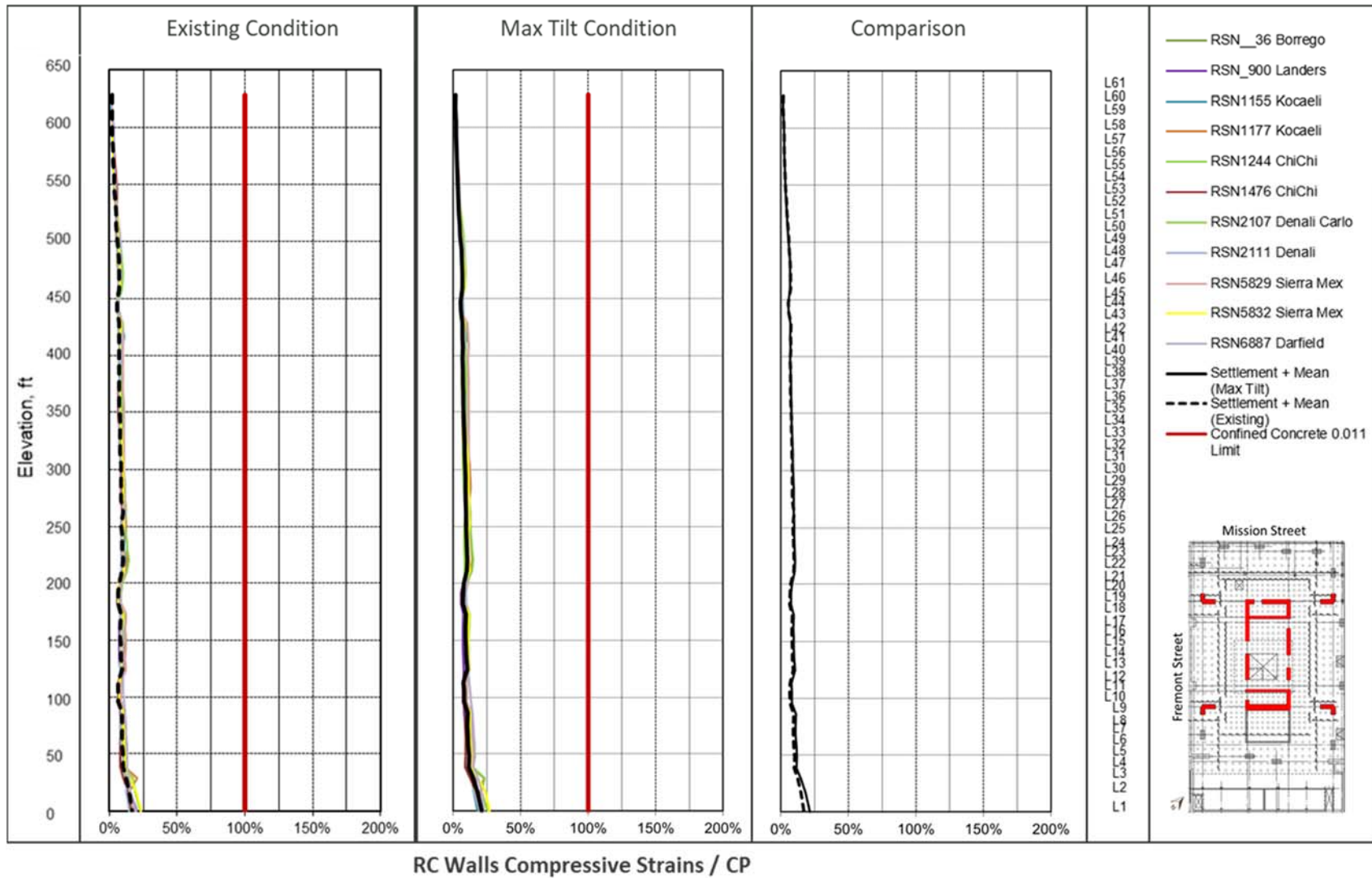


Figure 2-11 – East-West Peak Tower Foundation Displacements due to the MCE

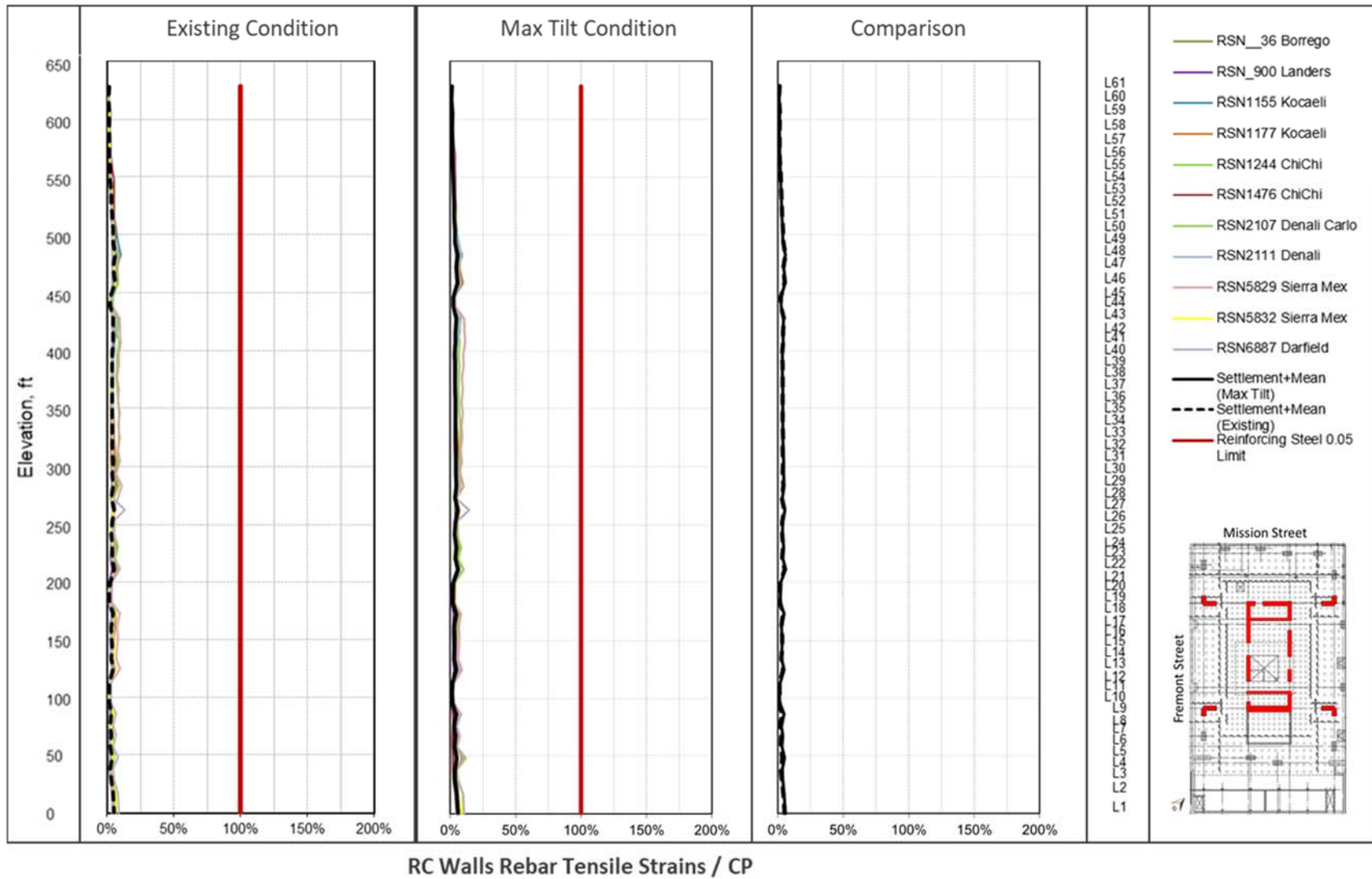
2.5 Superstructure Analysis Results

The sections below include plots of all force and deformation-controlled limit states from the analyses of the existing conditions and the 3.5 times the current tilt models. At 3.5 times the current tilt the superstructure behavior remains acceptable.

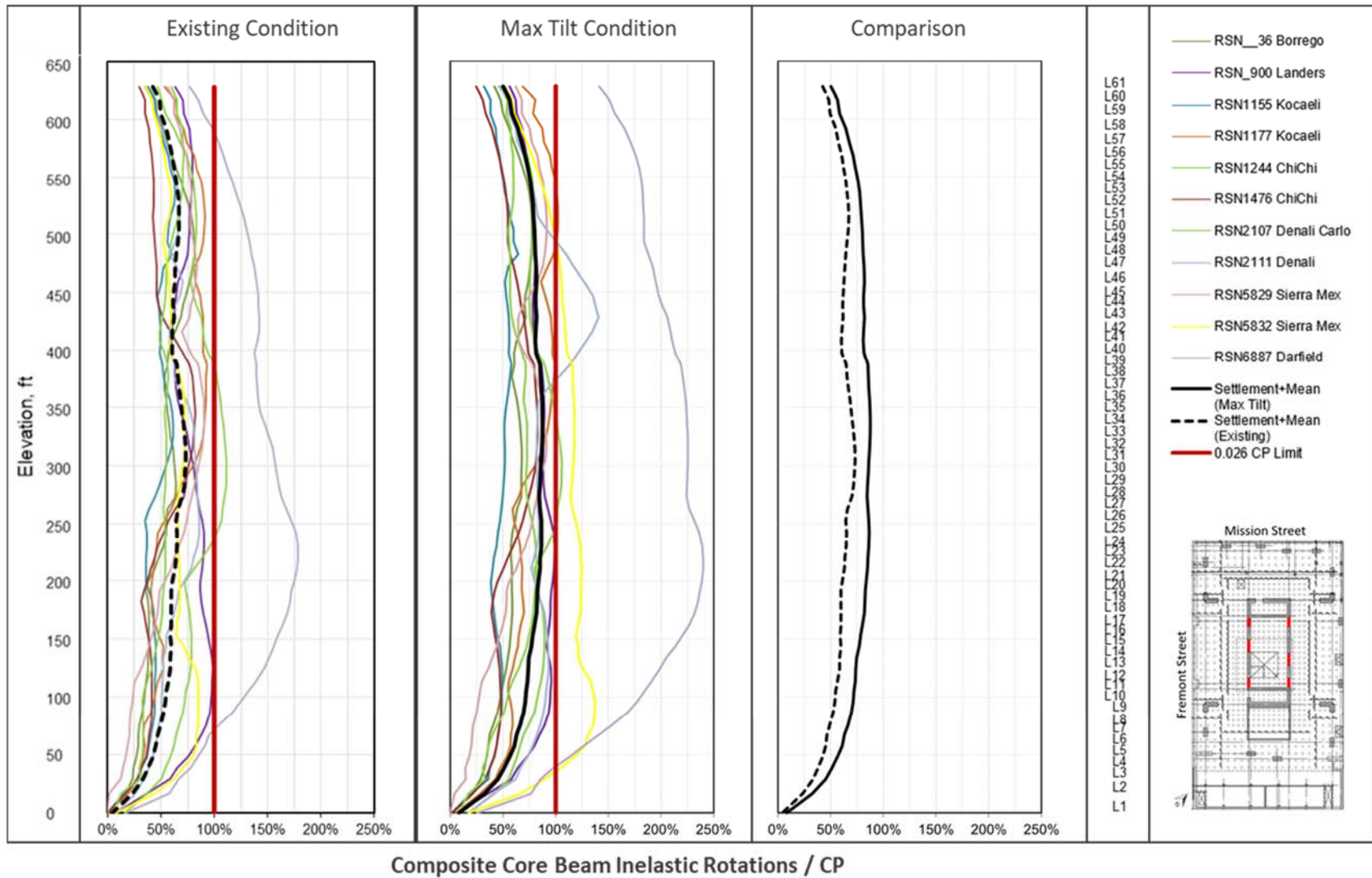
2.5.1 Shear Wall Concrete Compressive Strains



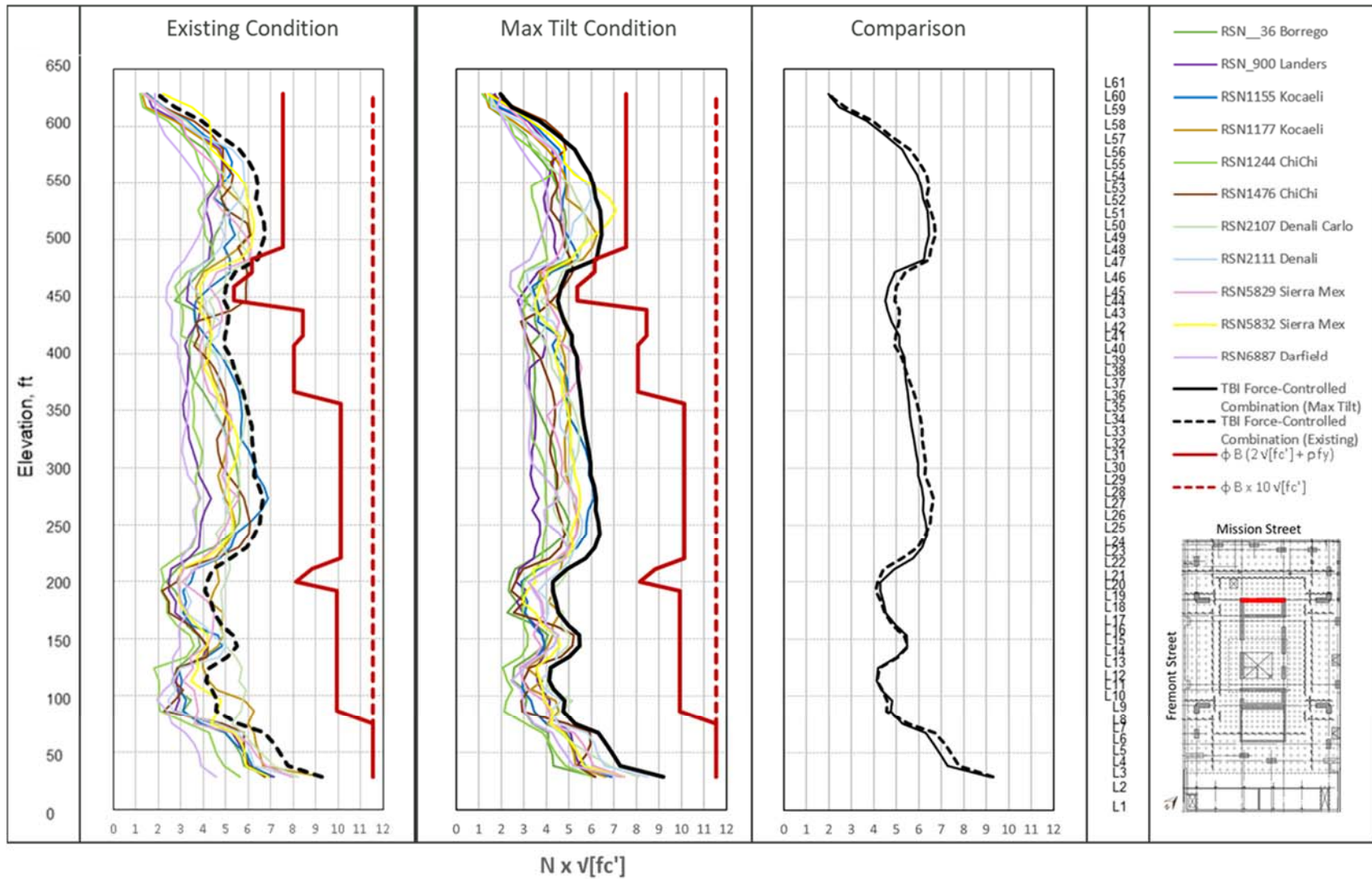
2.5.2 Shear Wall Steel Tensile Strains

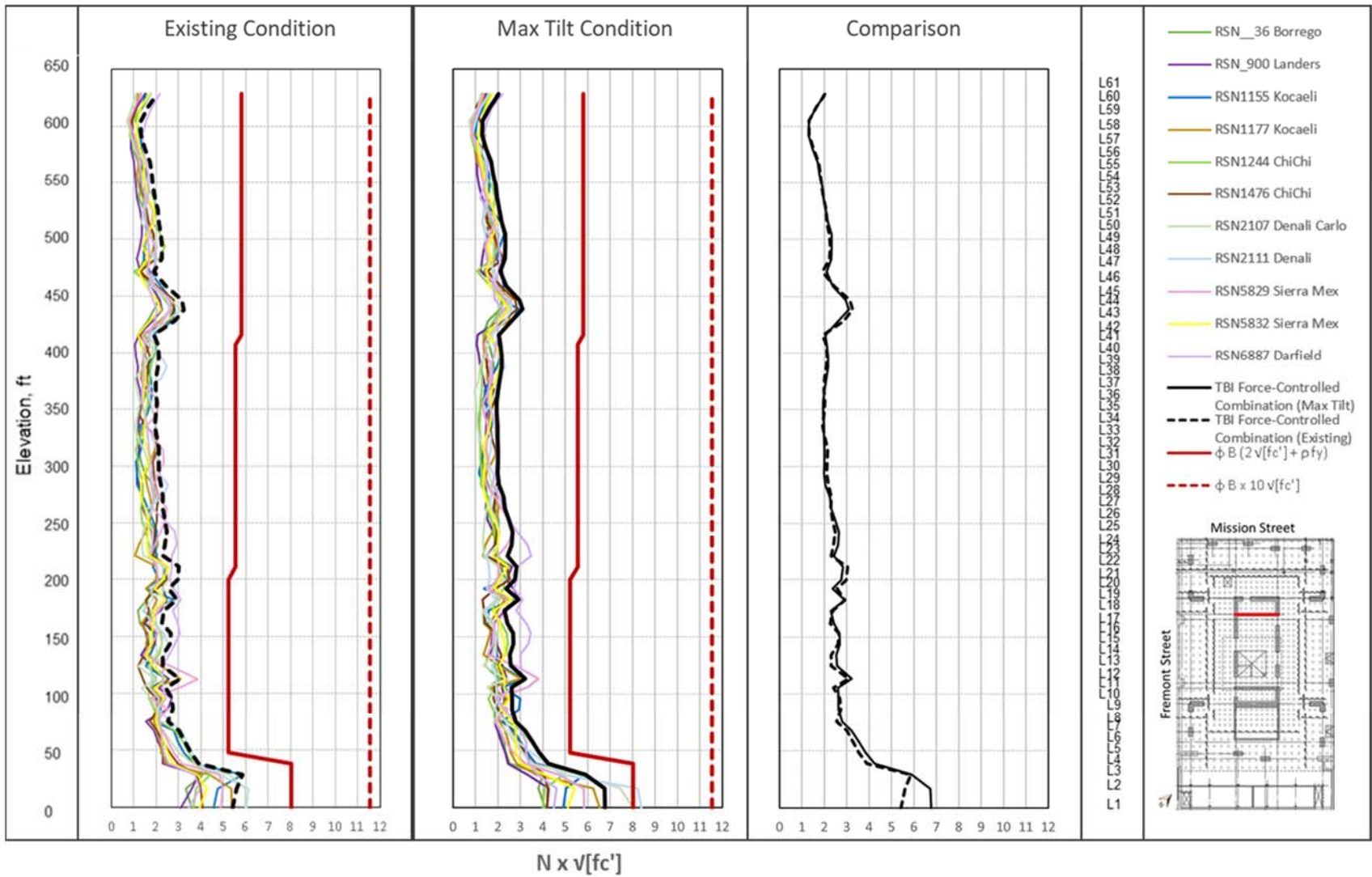


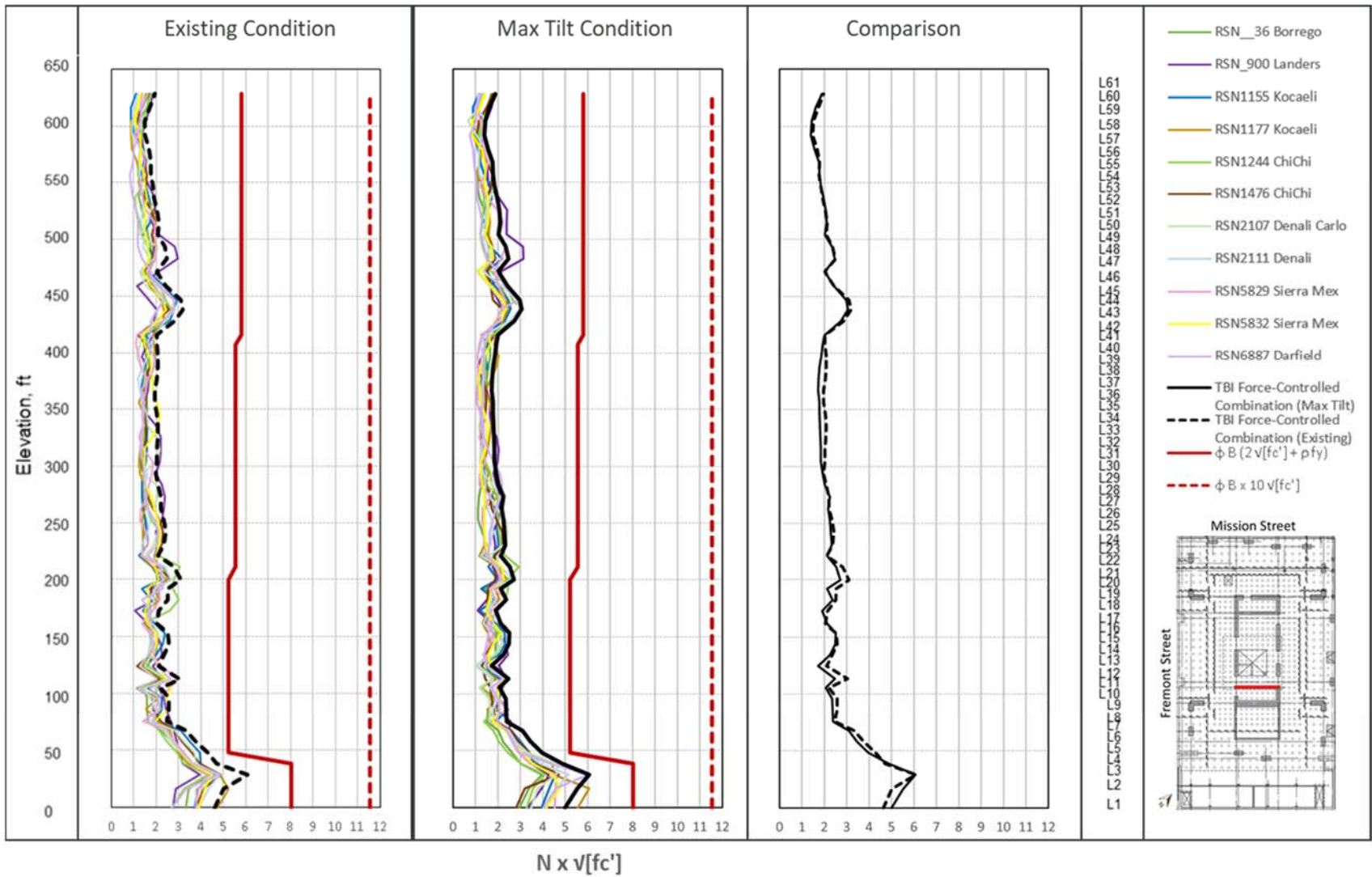
2.5.3 Composite Coupling Beam Inelastic Rotations

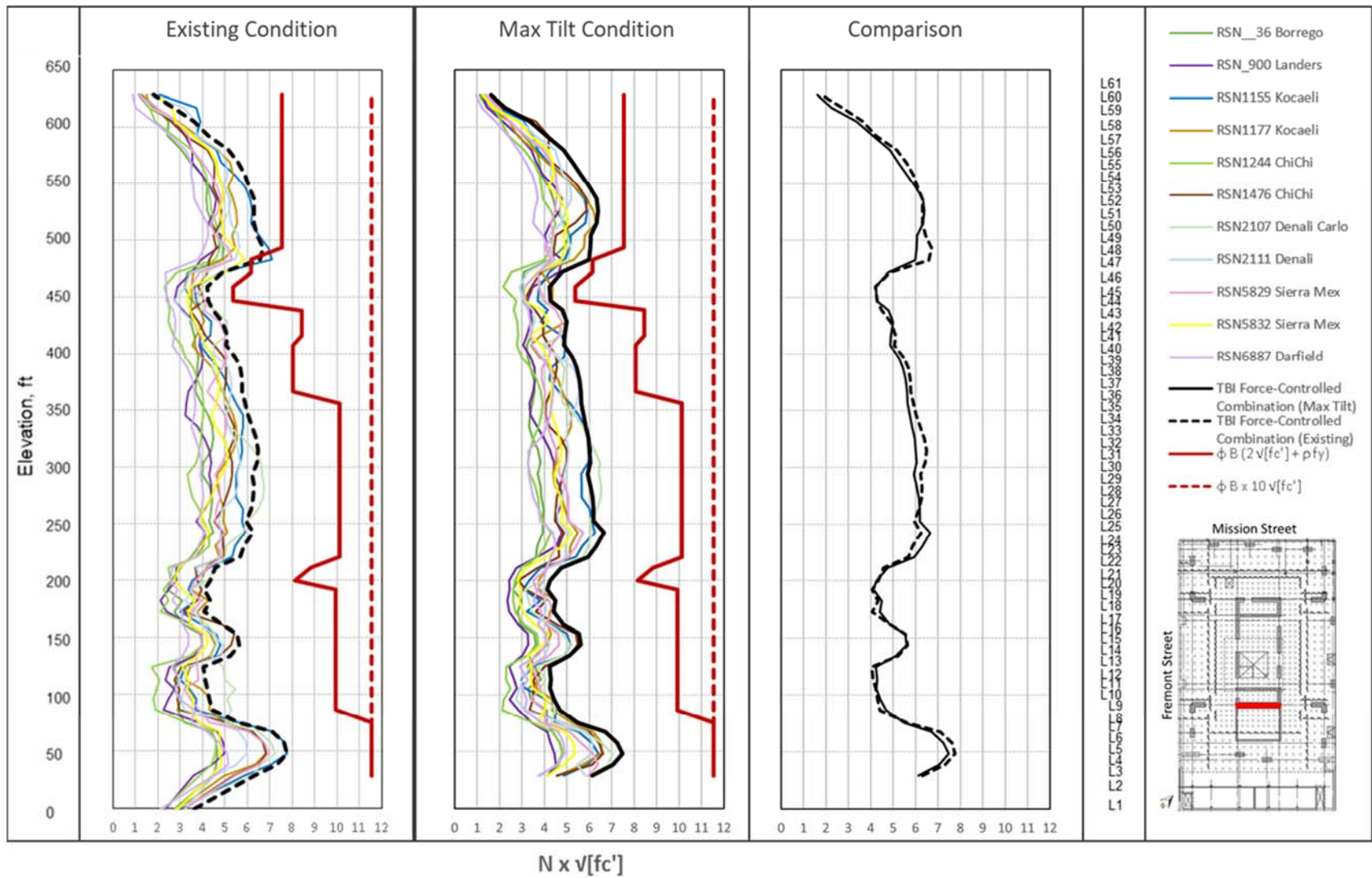


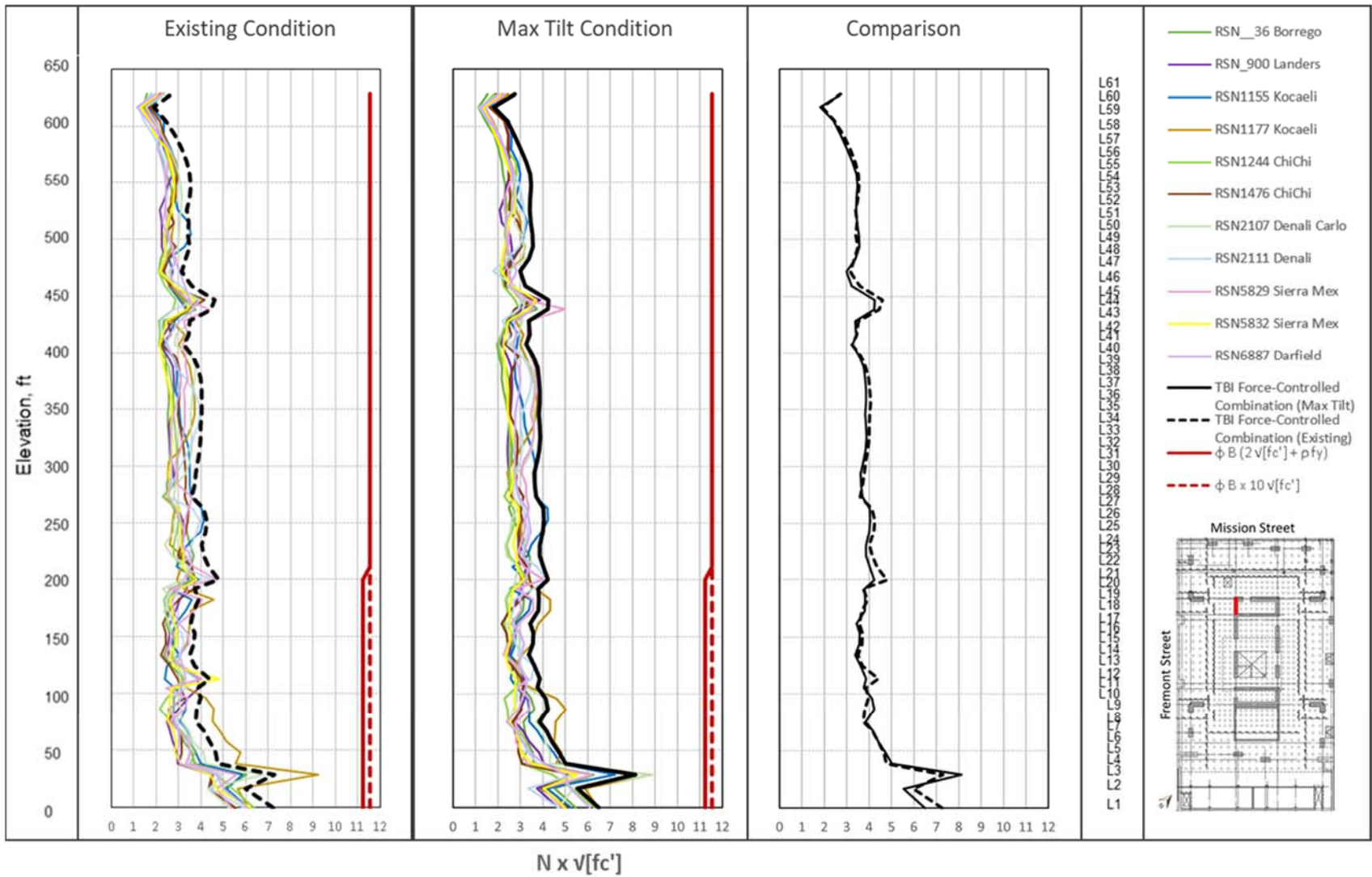
2.5.4 Shear Wall Forces

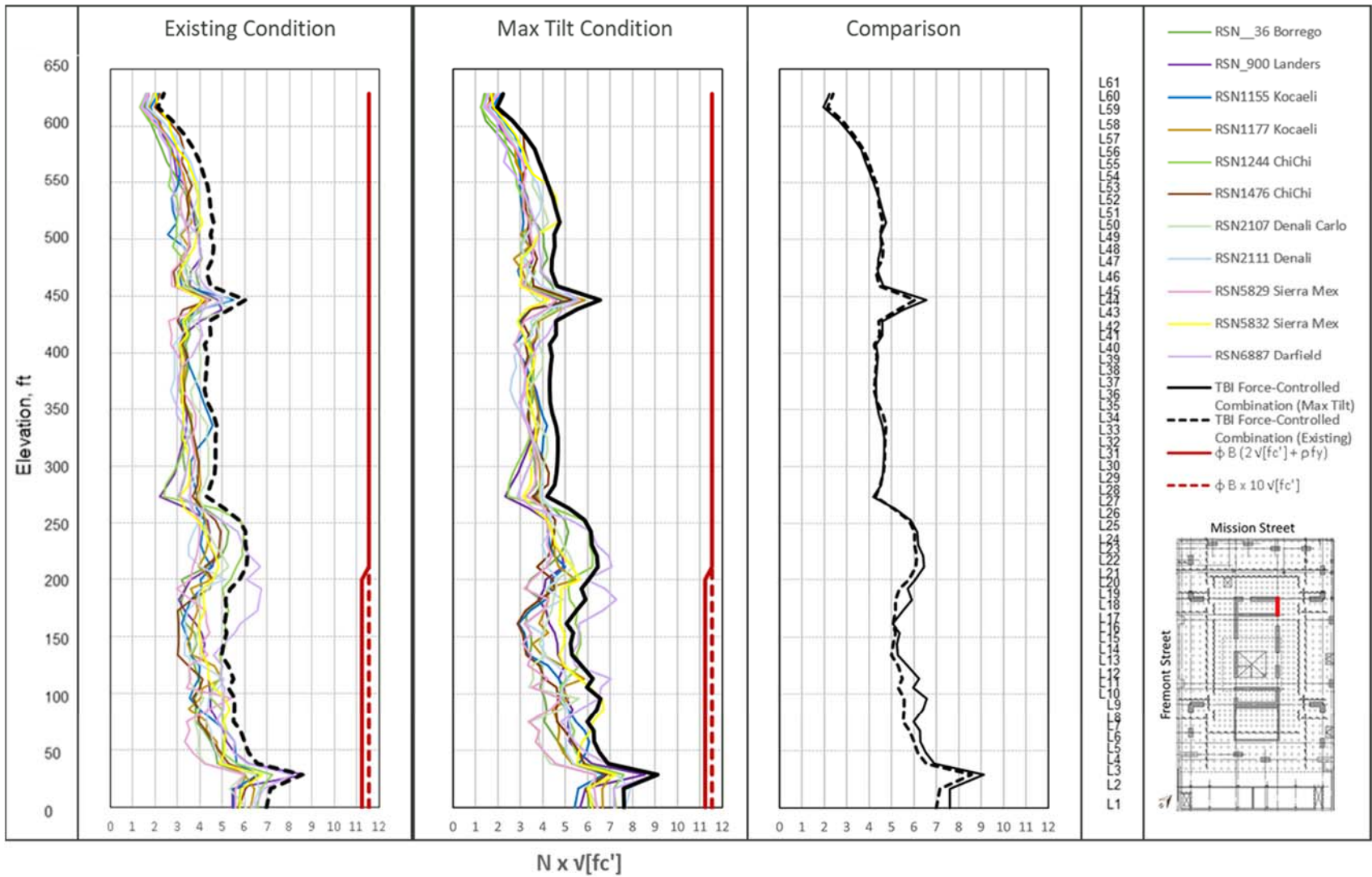


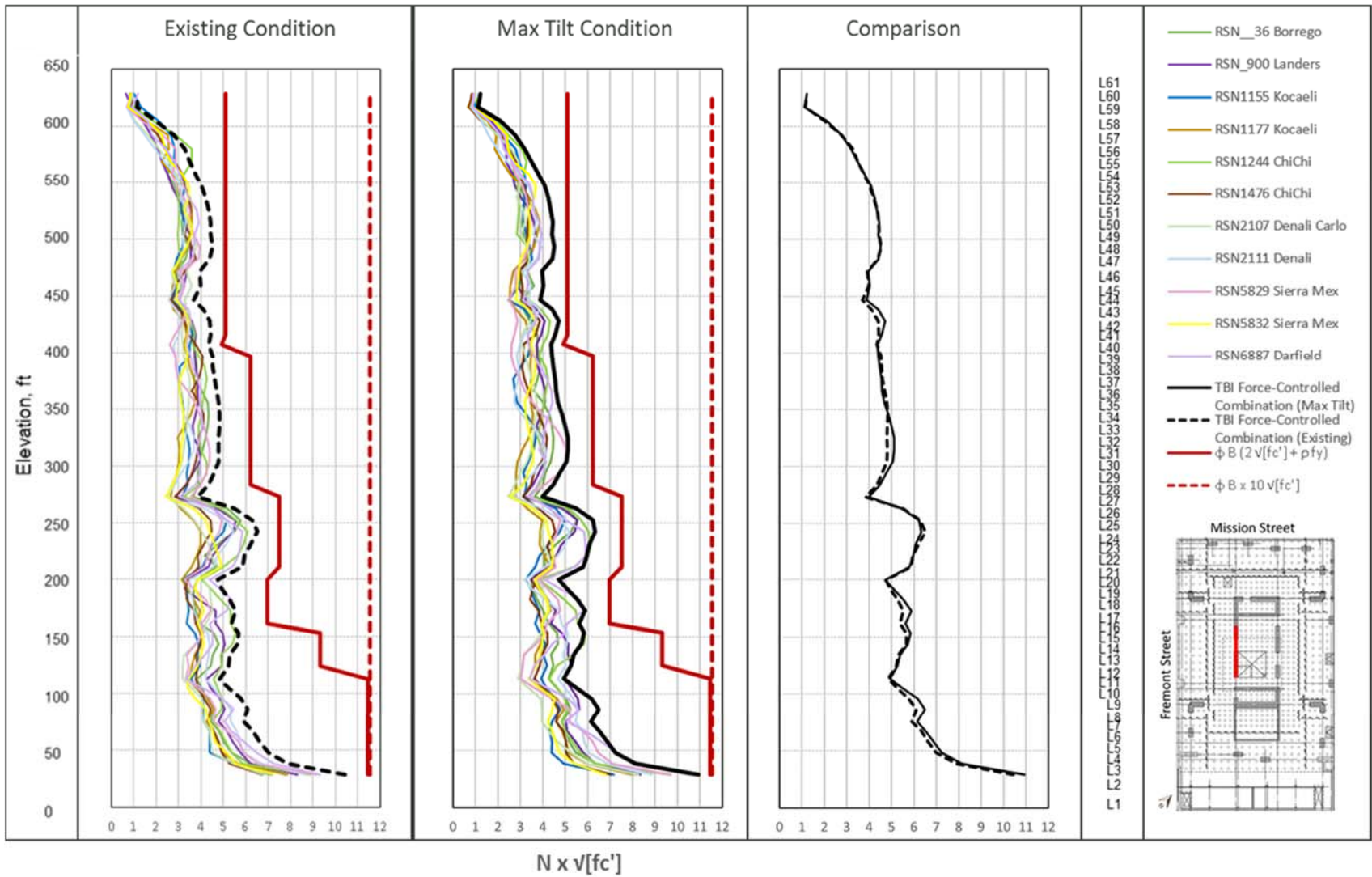


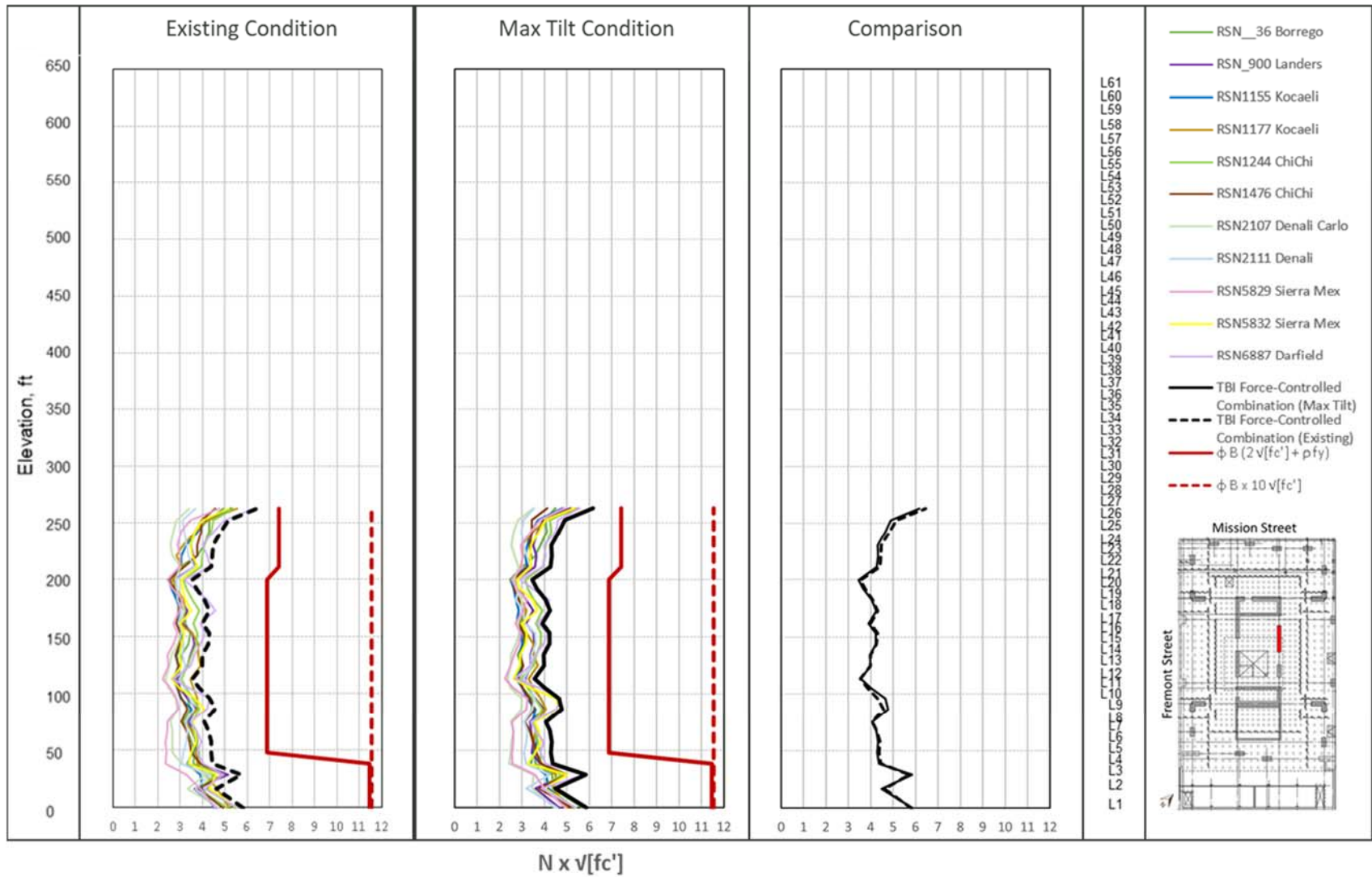


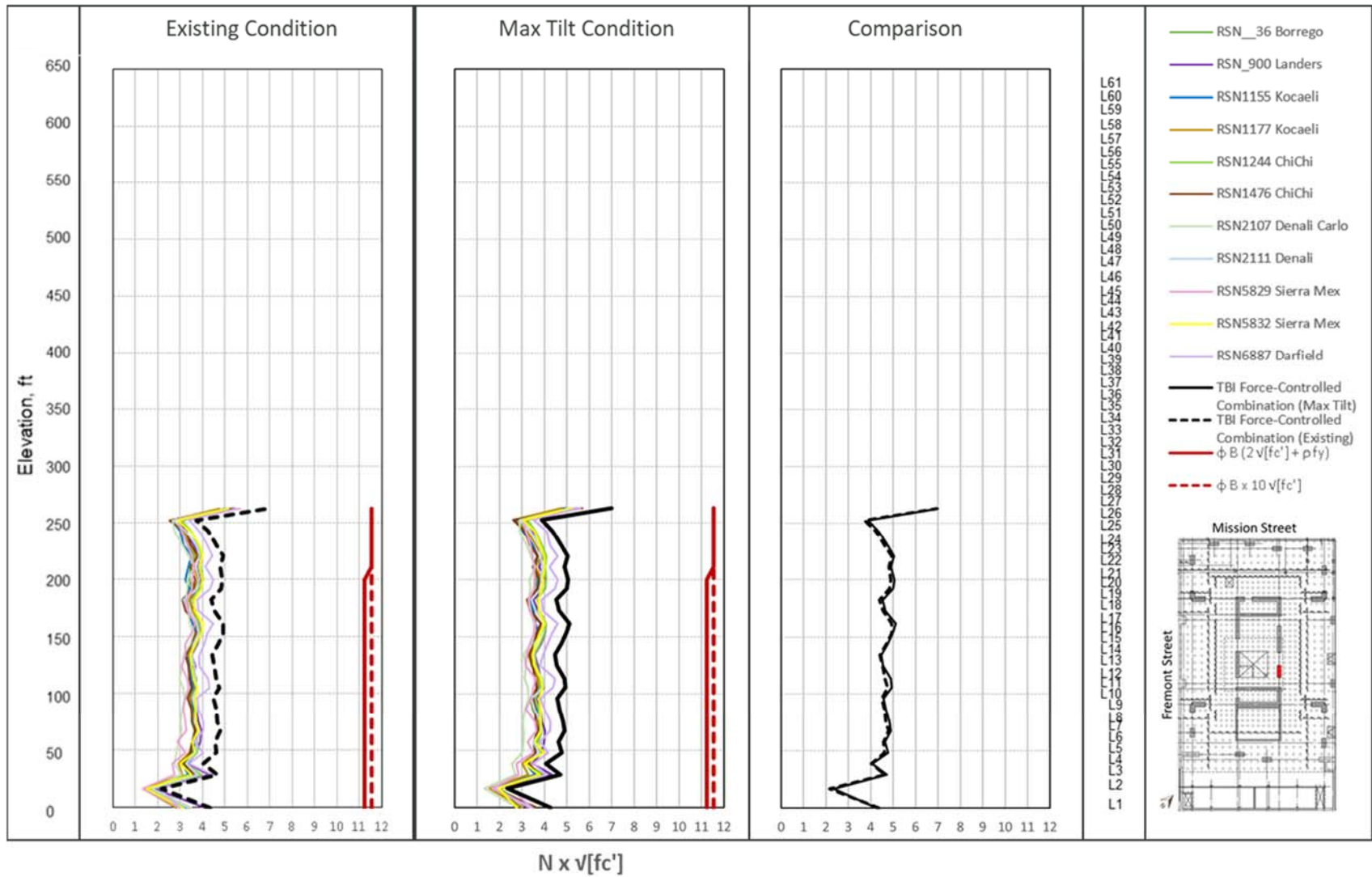


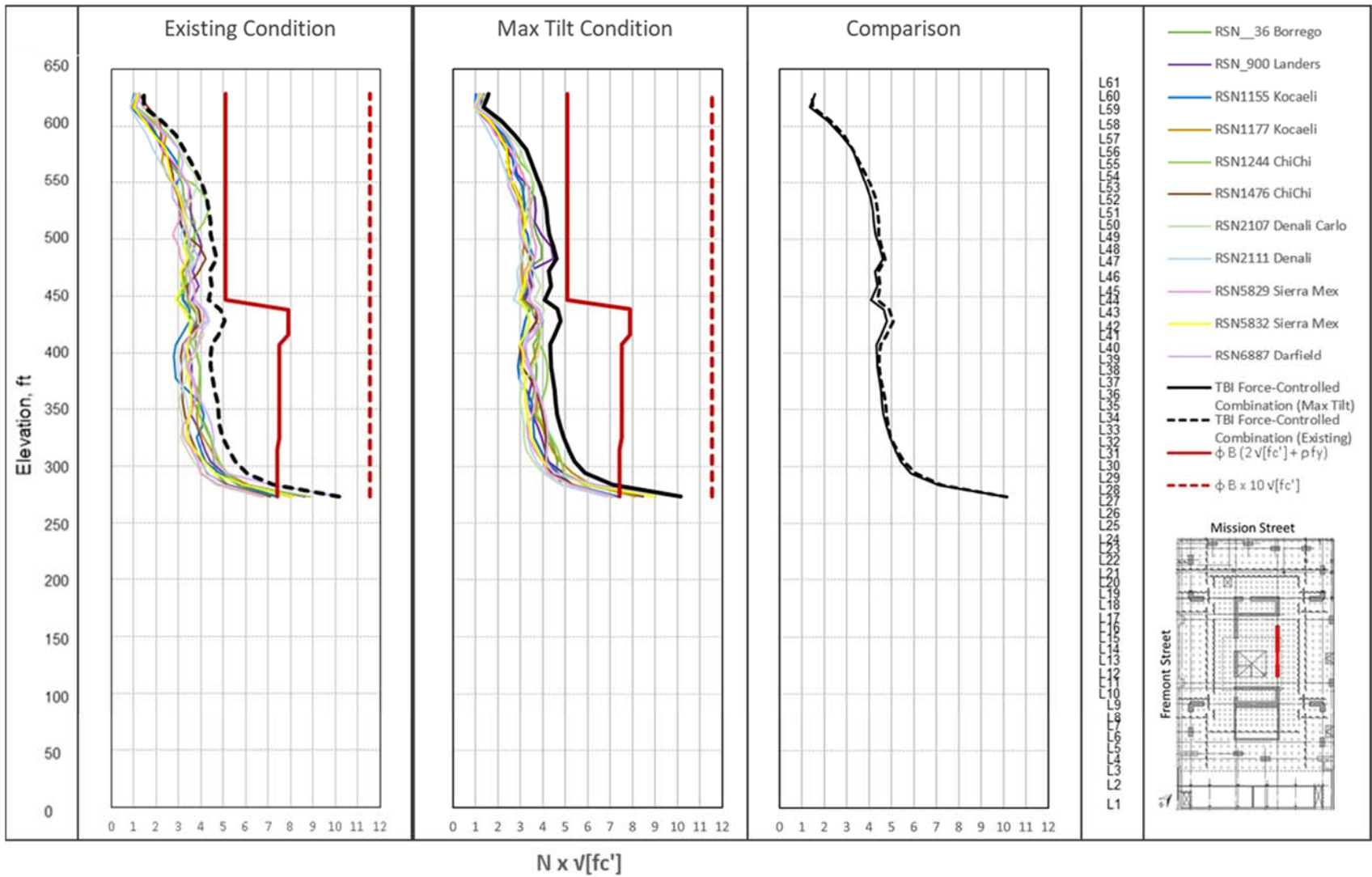


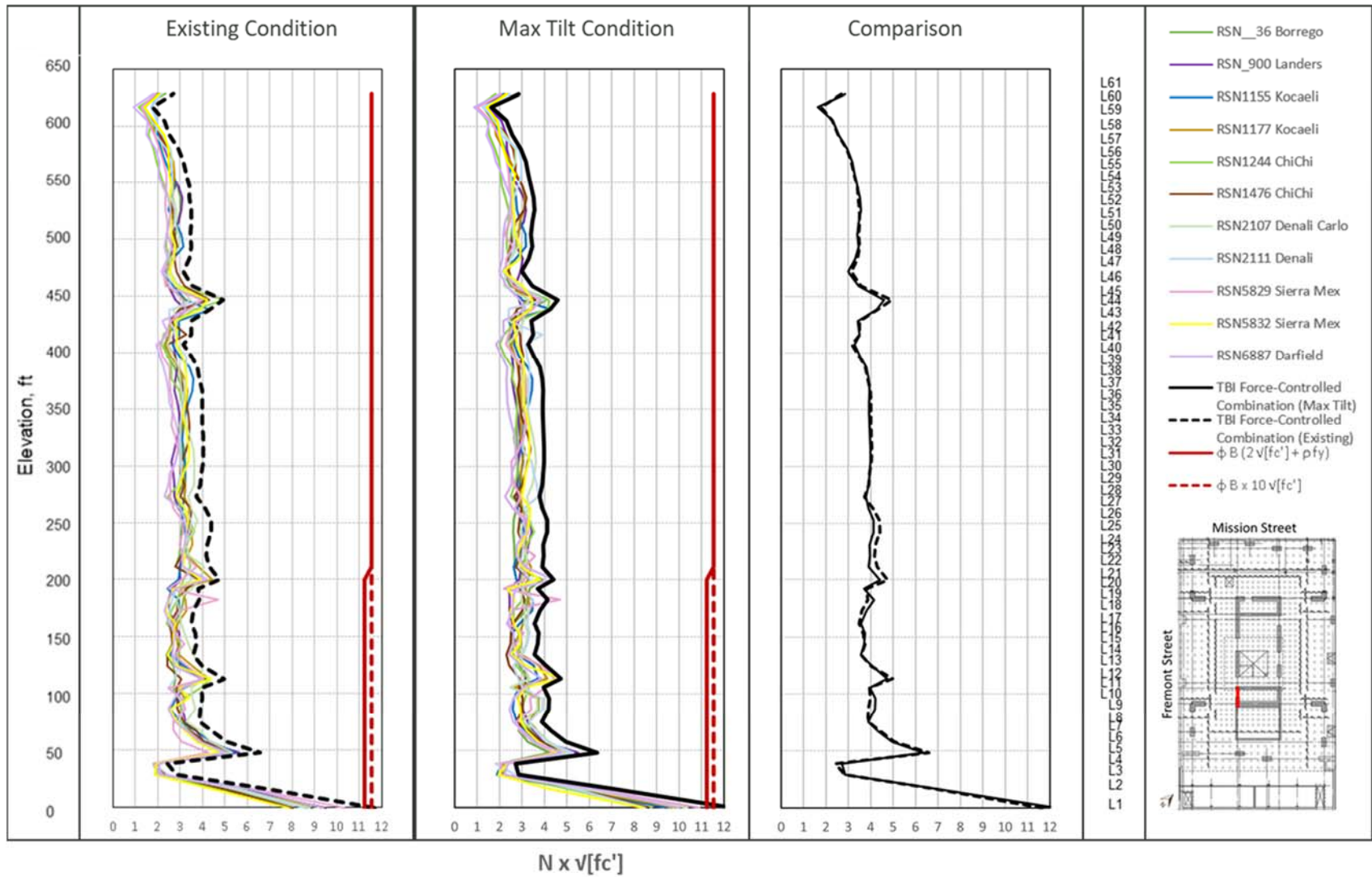


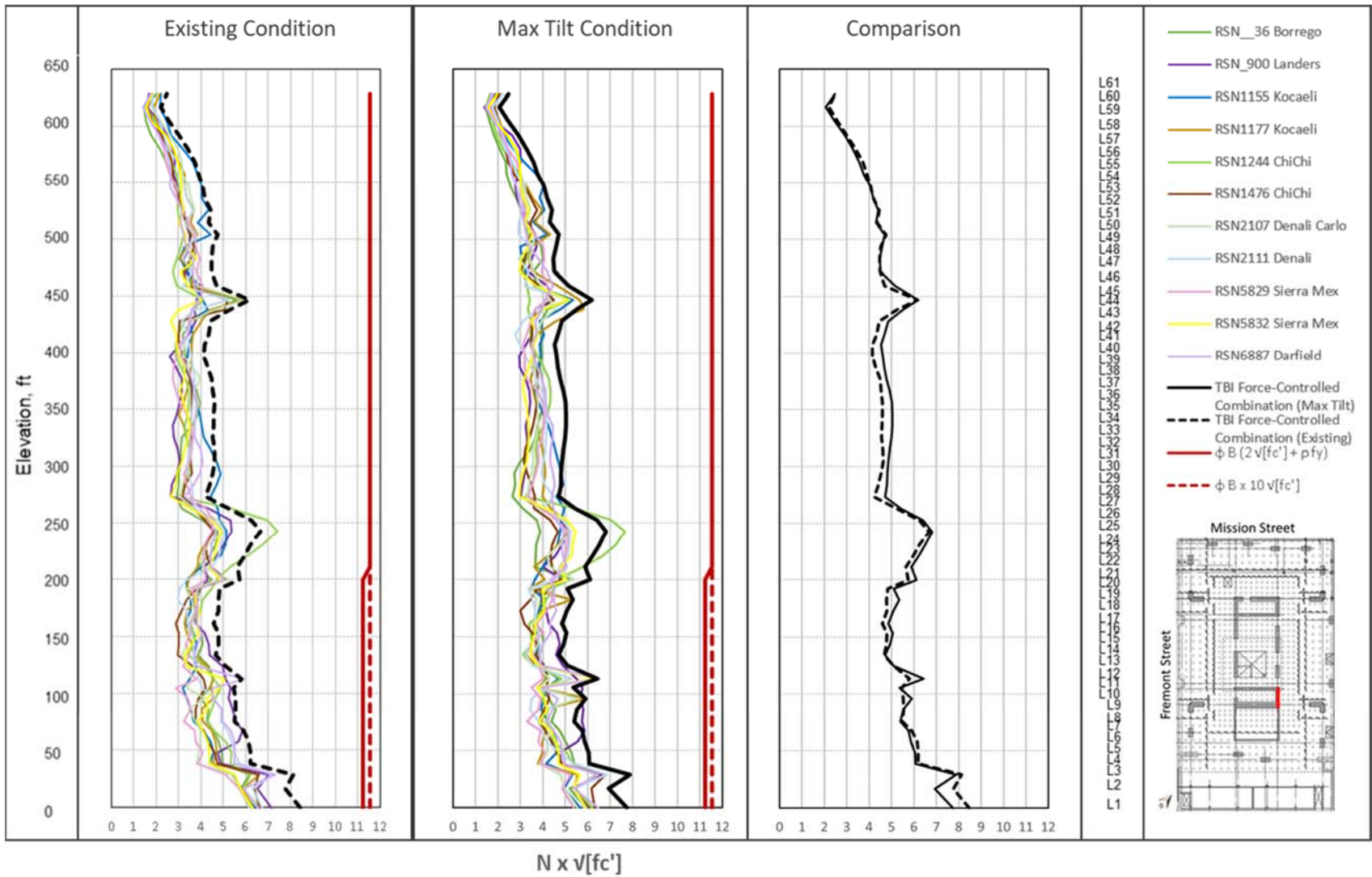


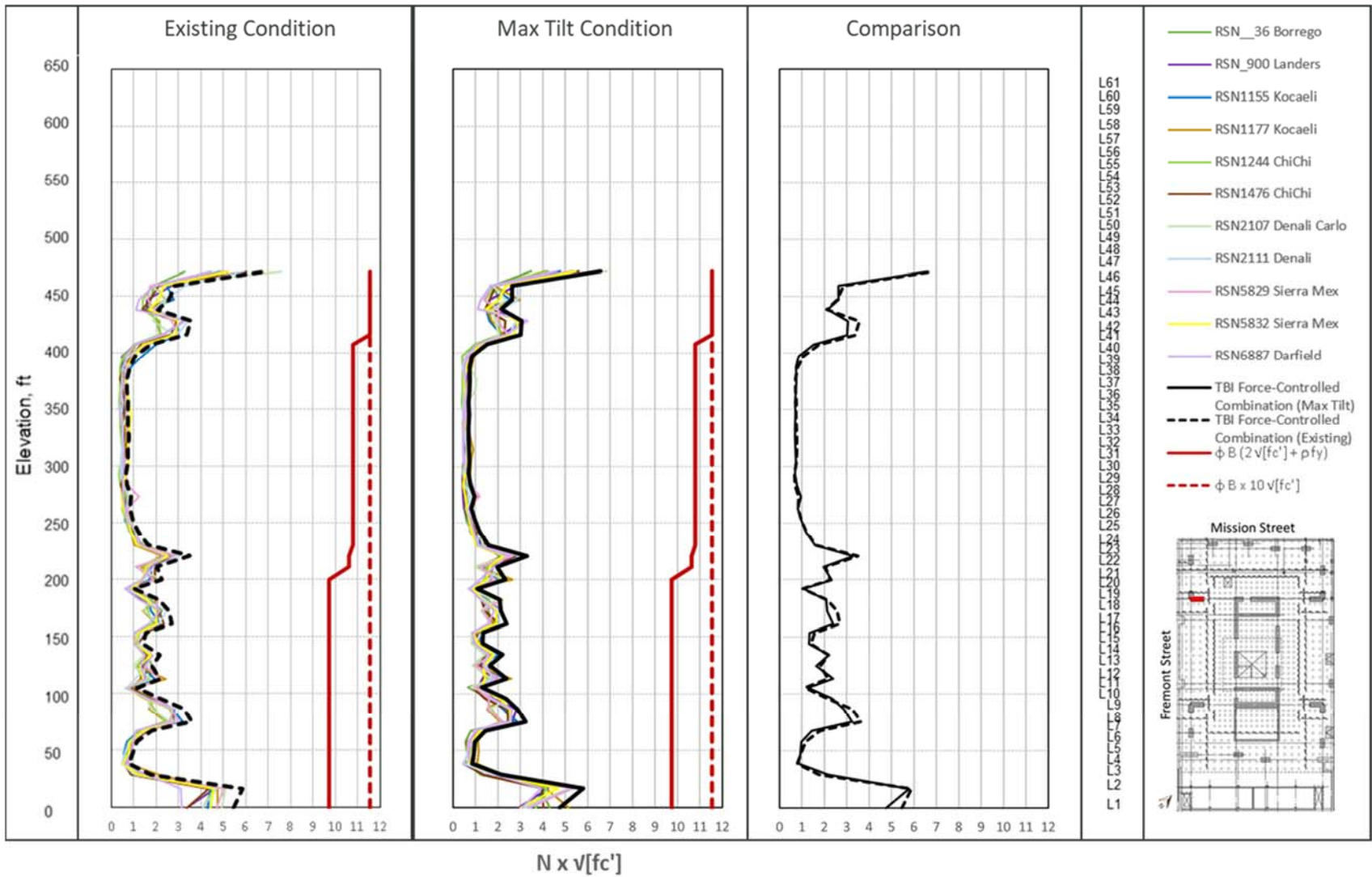


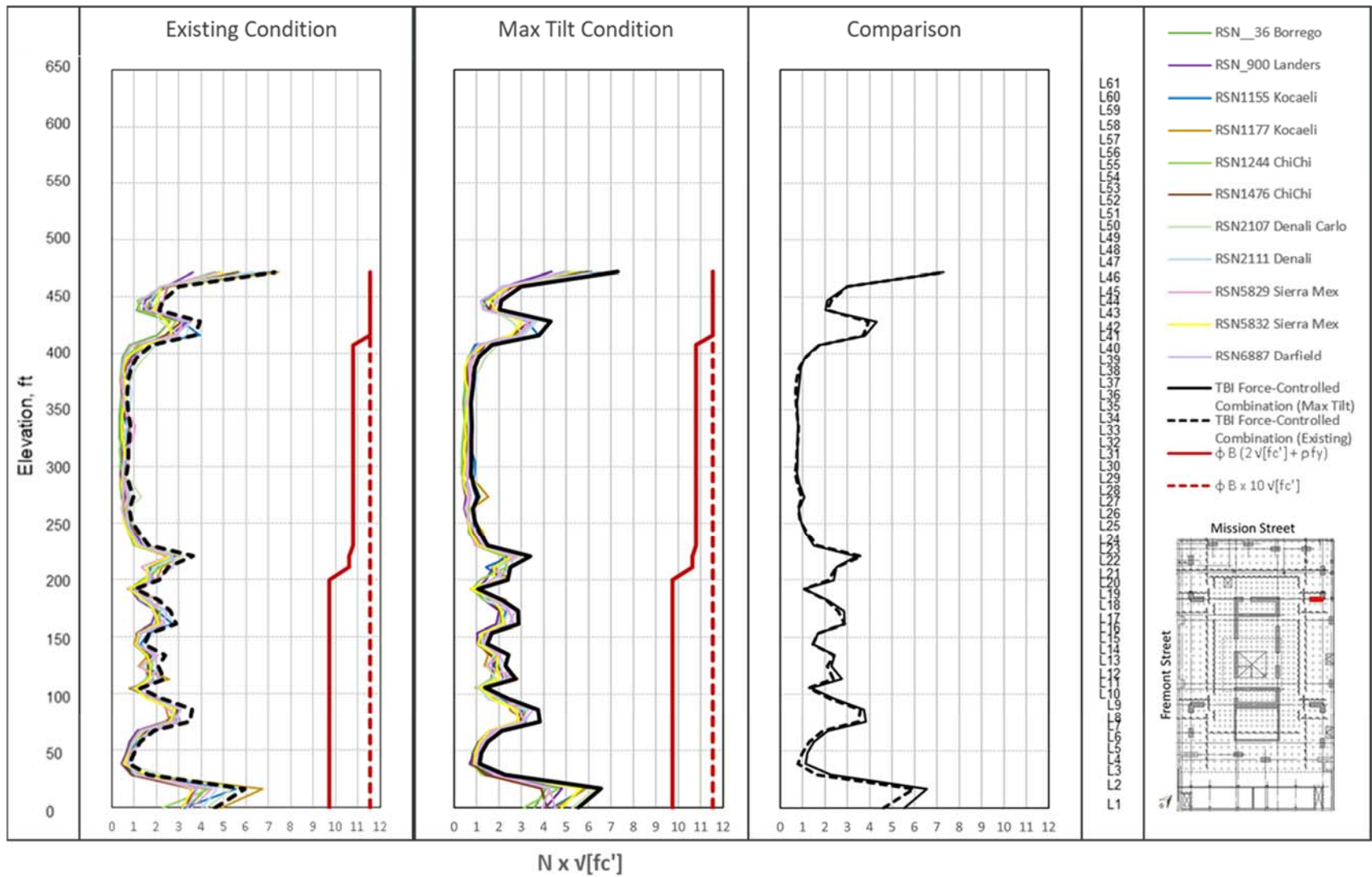


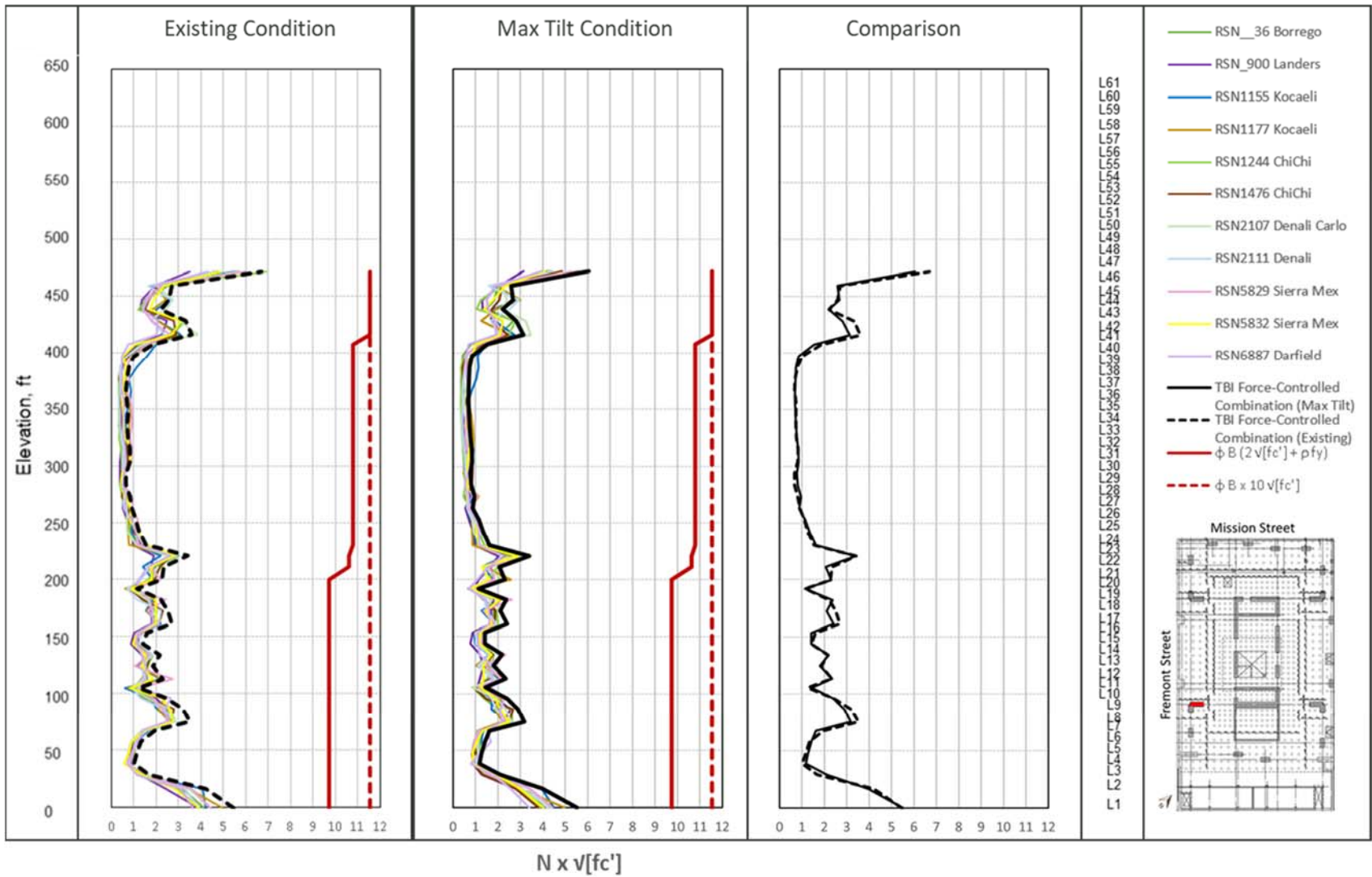


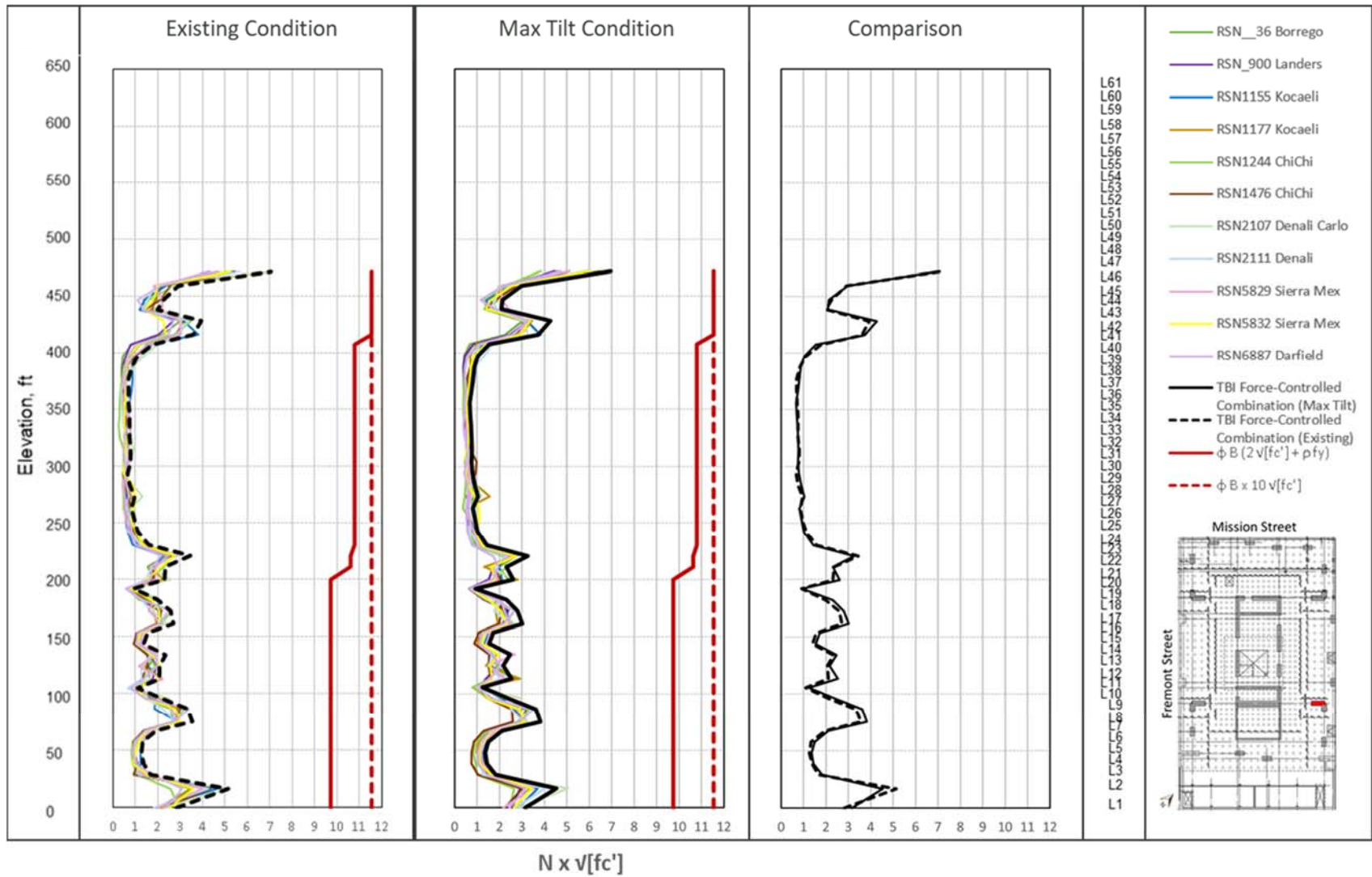


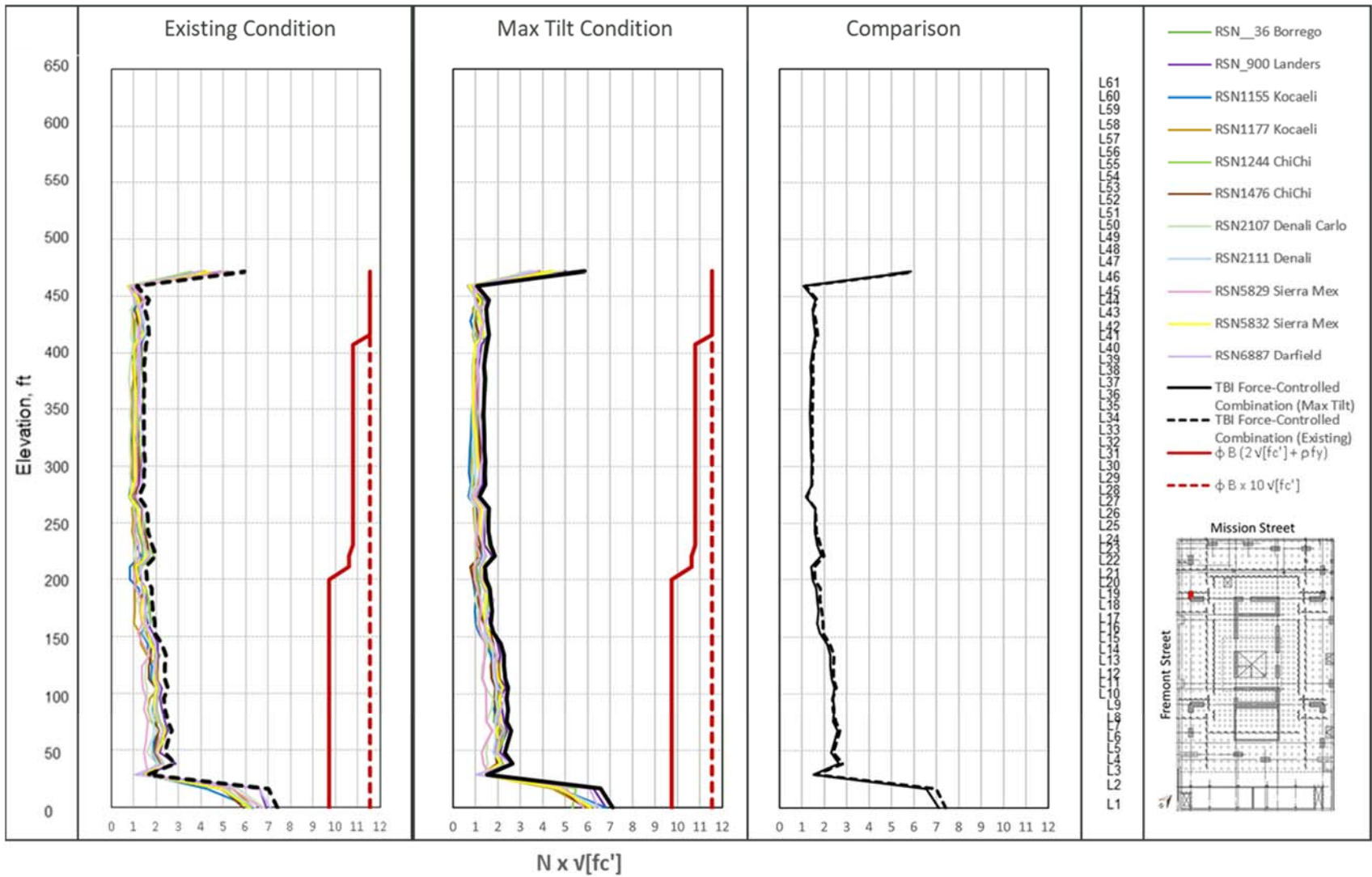


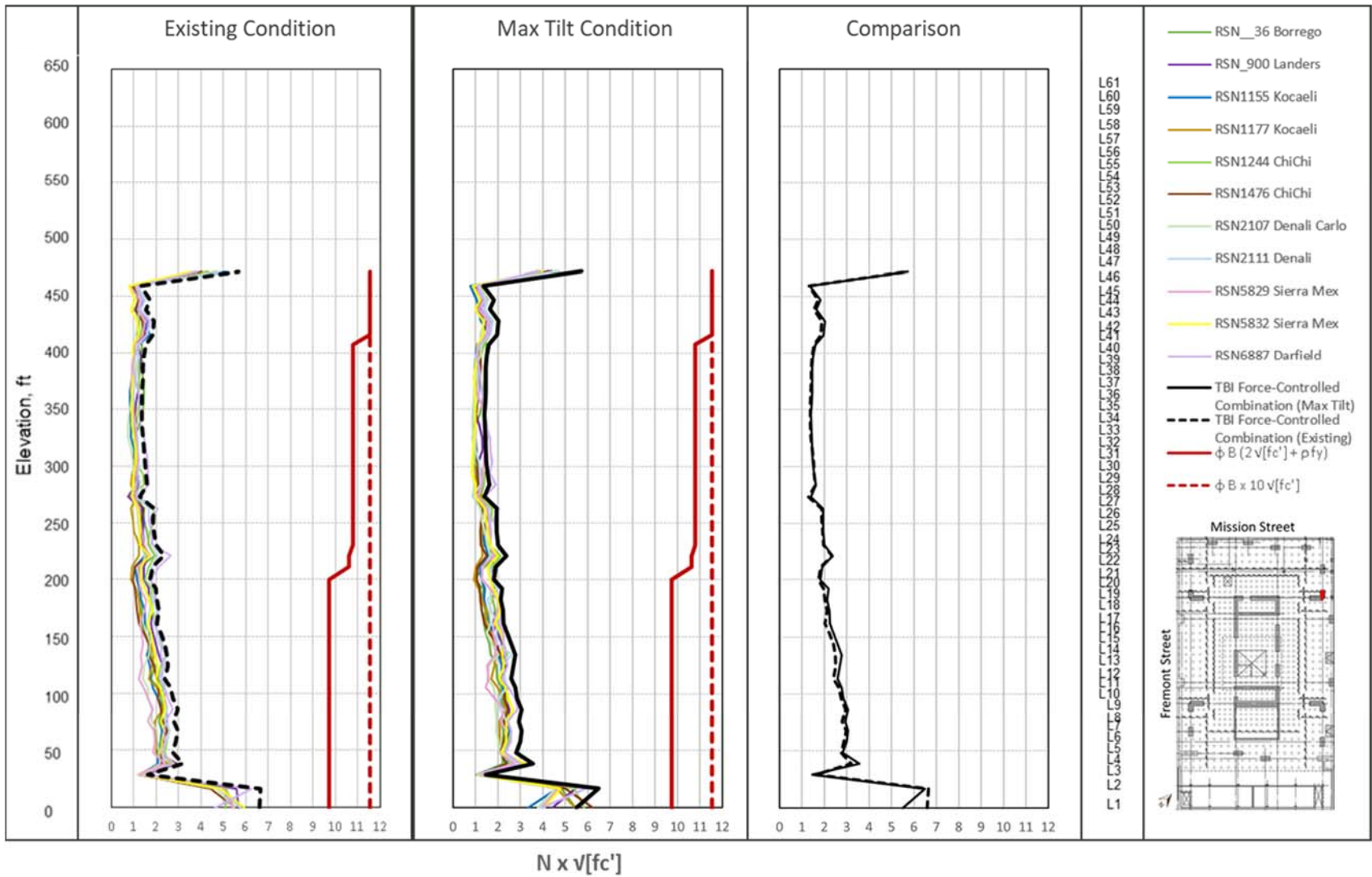


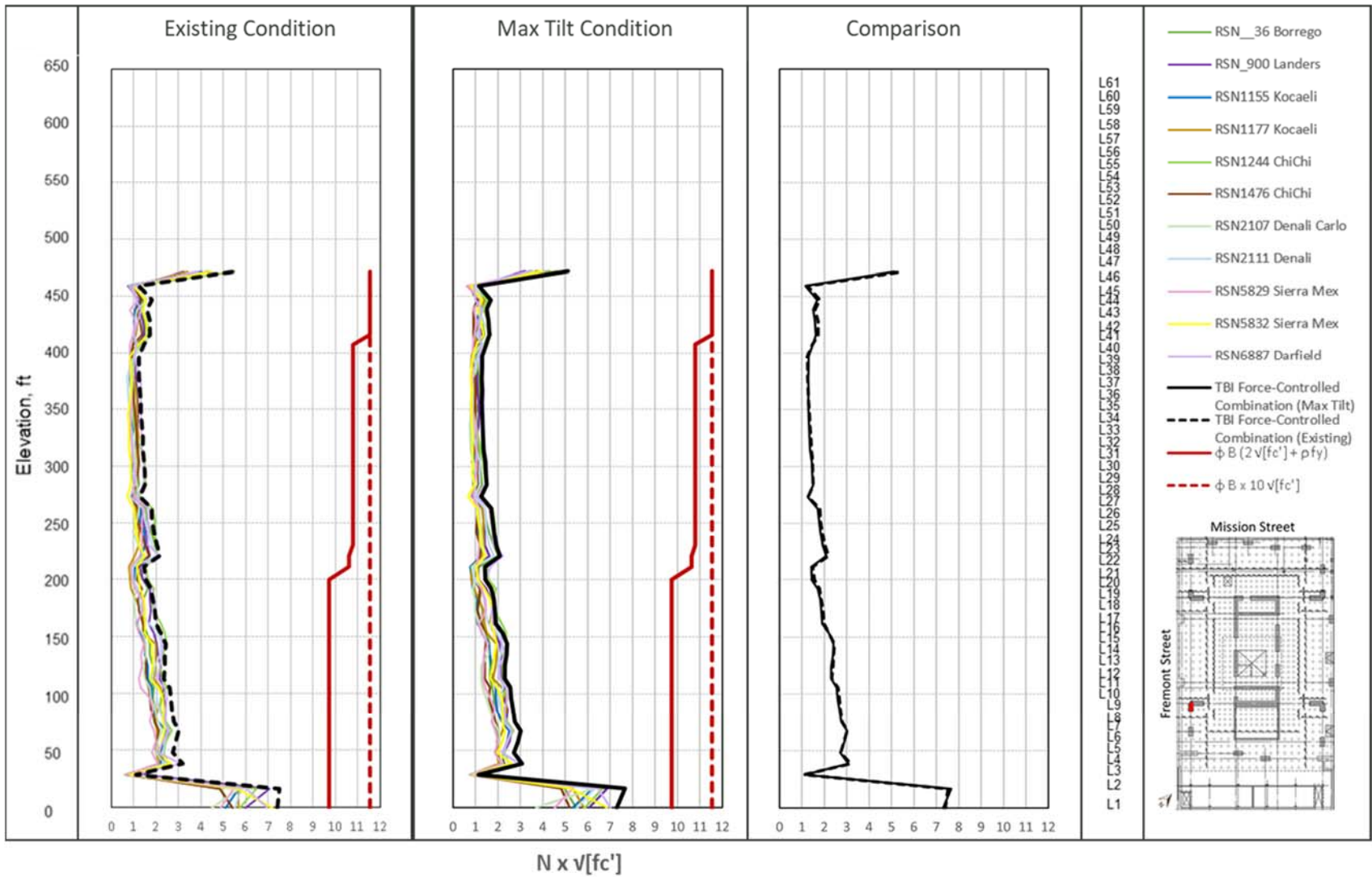


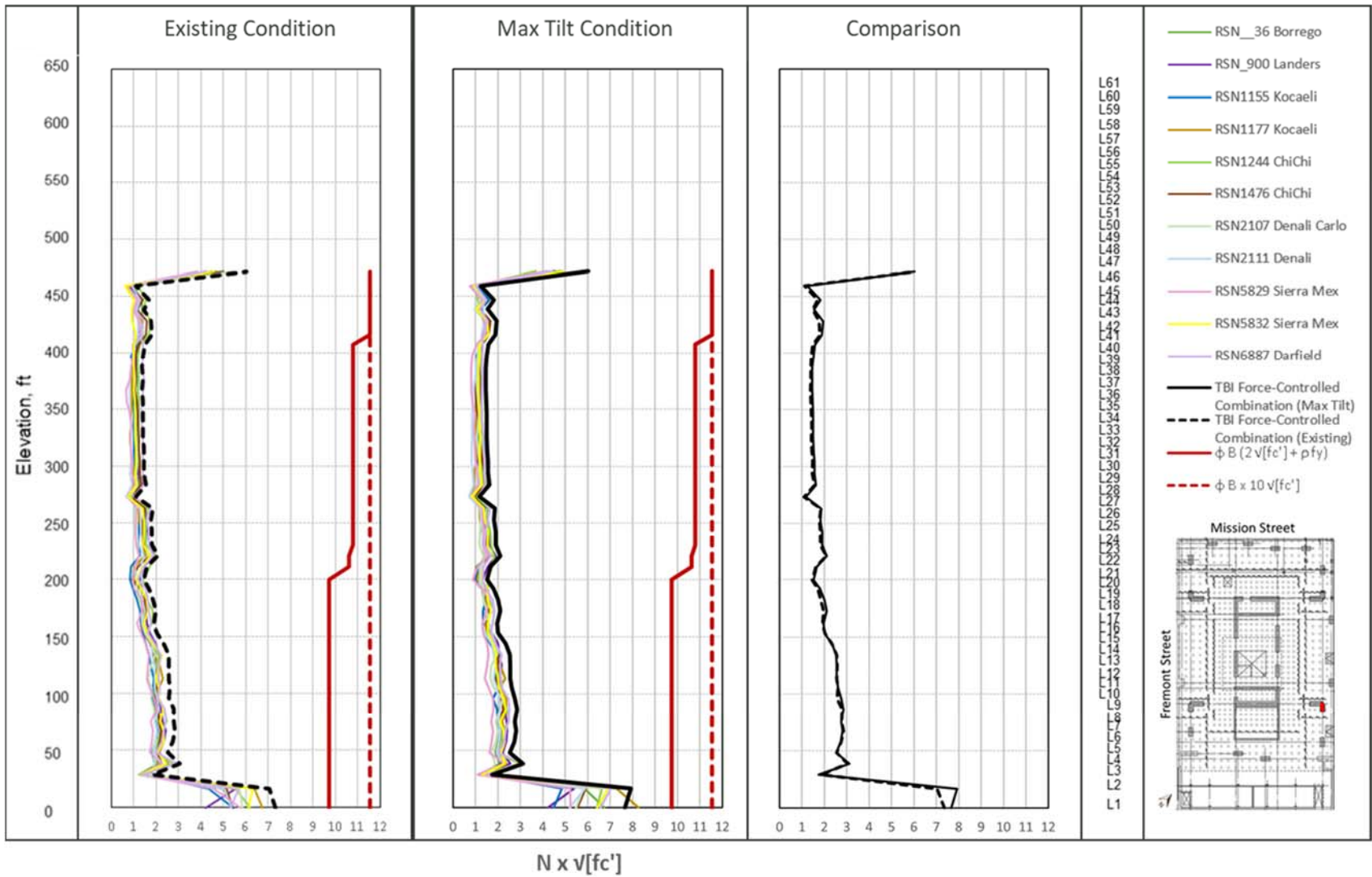








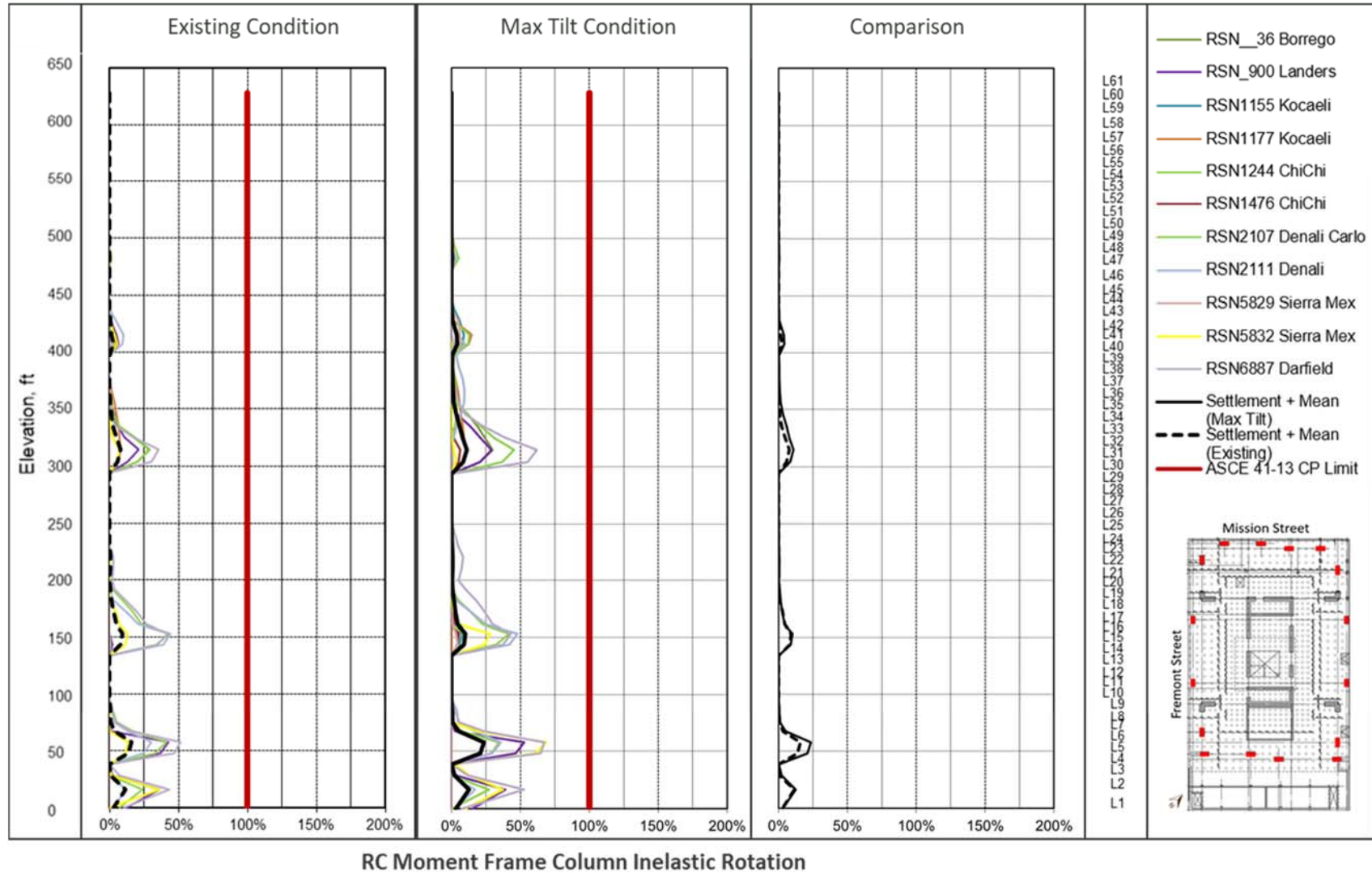




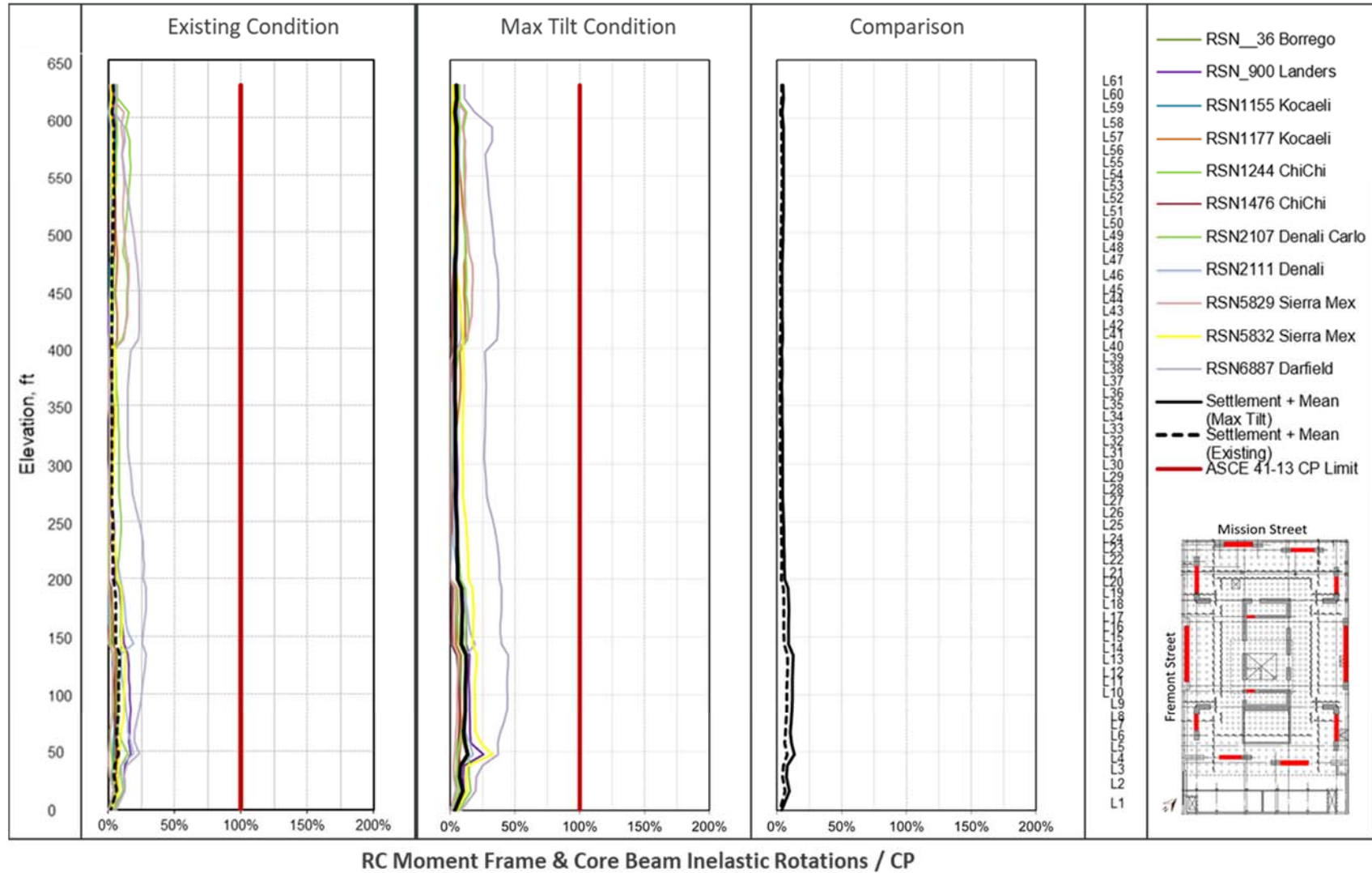
1 and 2-story wall piers. Force-controlled load combination:

Shear Wall	Exiting Condition Demand ($\sqrt{f'c}$)	Max Tilt Condition Demand ($\sqrt{f'c}$)	Capacity ($\sqrt{f'c}$)
SW_LineC-4_LB1	2.2	2.4	11.5
SW_LineC-4_L1	2.5	2.5	11.5
SW_LineC-9_LB1	3.4	3.7	11.5
SW_LineC-9_L1	5.4	6.0	11.5
SW_LineF-4	4.8	5.4	11.5
SW_LineF-9	4.8	4.0	11.5
SW_Line4-D_LB1	4.9	6.4	11.2
SW_Line4-D_L1	5.6	5.3	11.2
SW_Line4-E_LB1	5.3	5.5	11.5
SW_Line4-E_L1	5.2	5.8	11.5

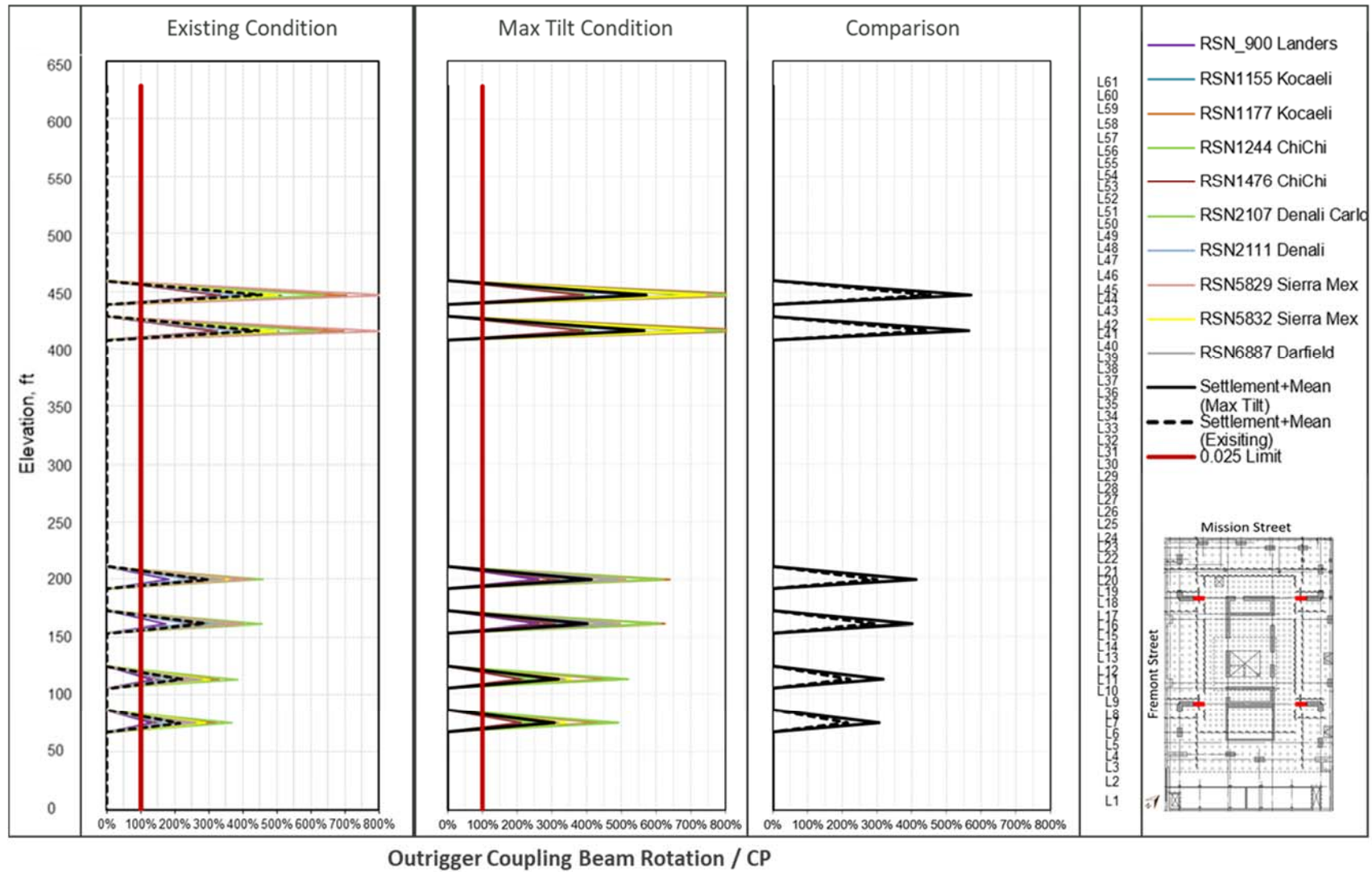
2.5.5 Moment Frame Column Plastic Rotations



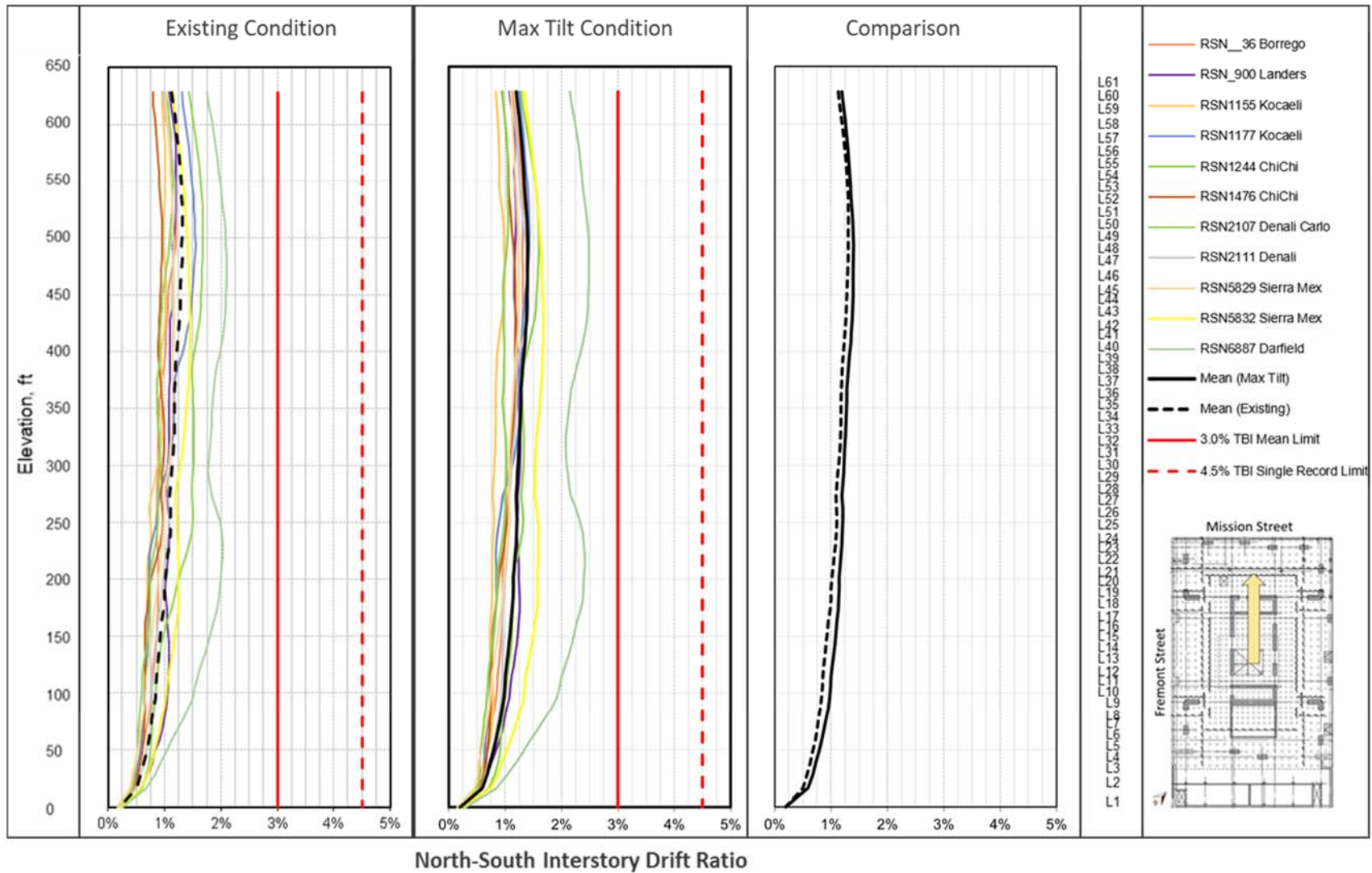
2.5.6 Moment Frame and Core Coupling Beam Plastic Rotations



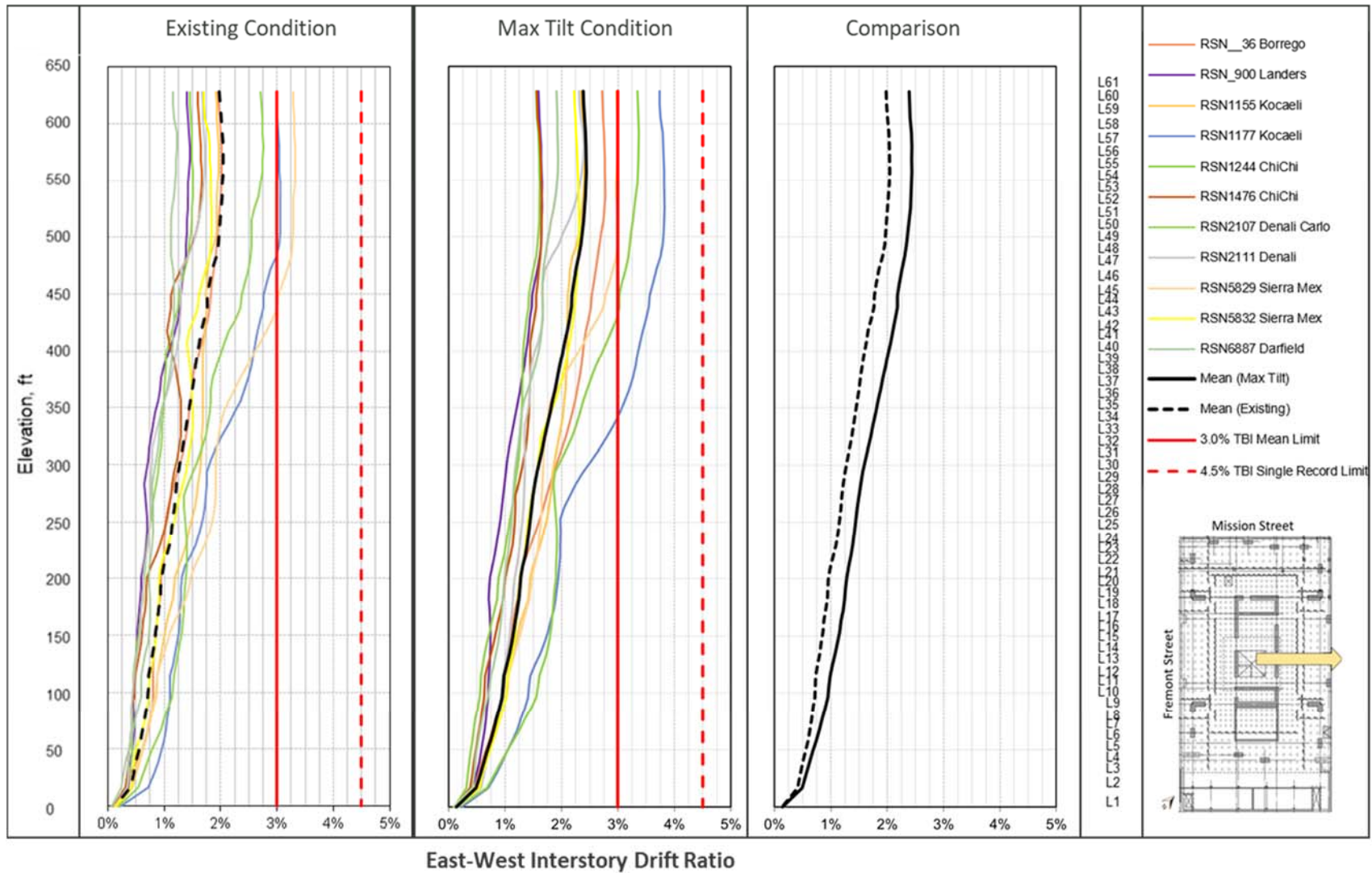
2.5.7 Outrigger Coupling Beam Rotations



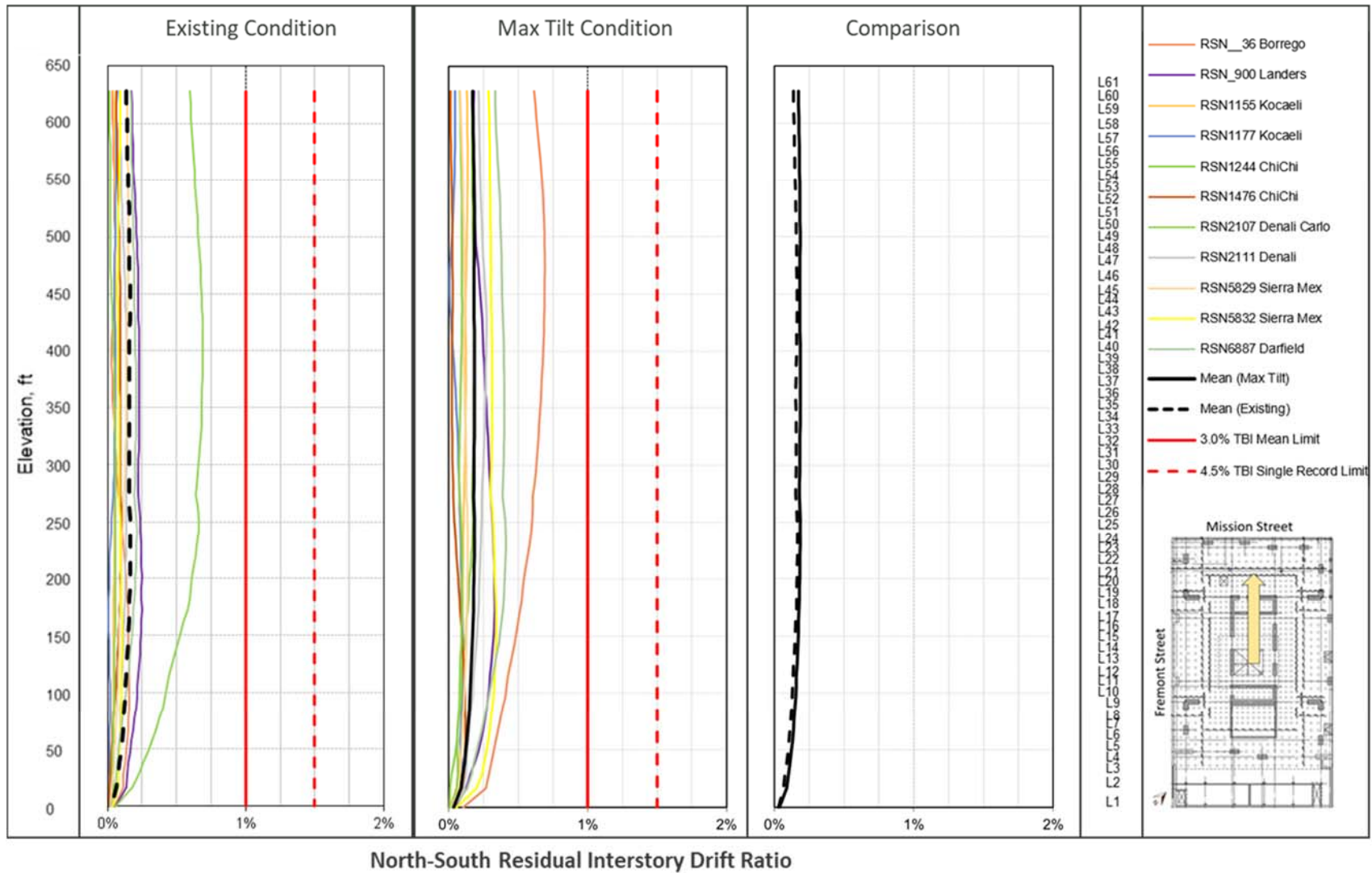
2.5.8 North-South Direction Seismic Transient Interstory Drift Ratios



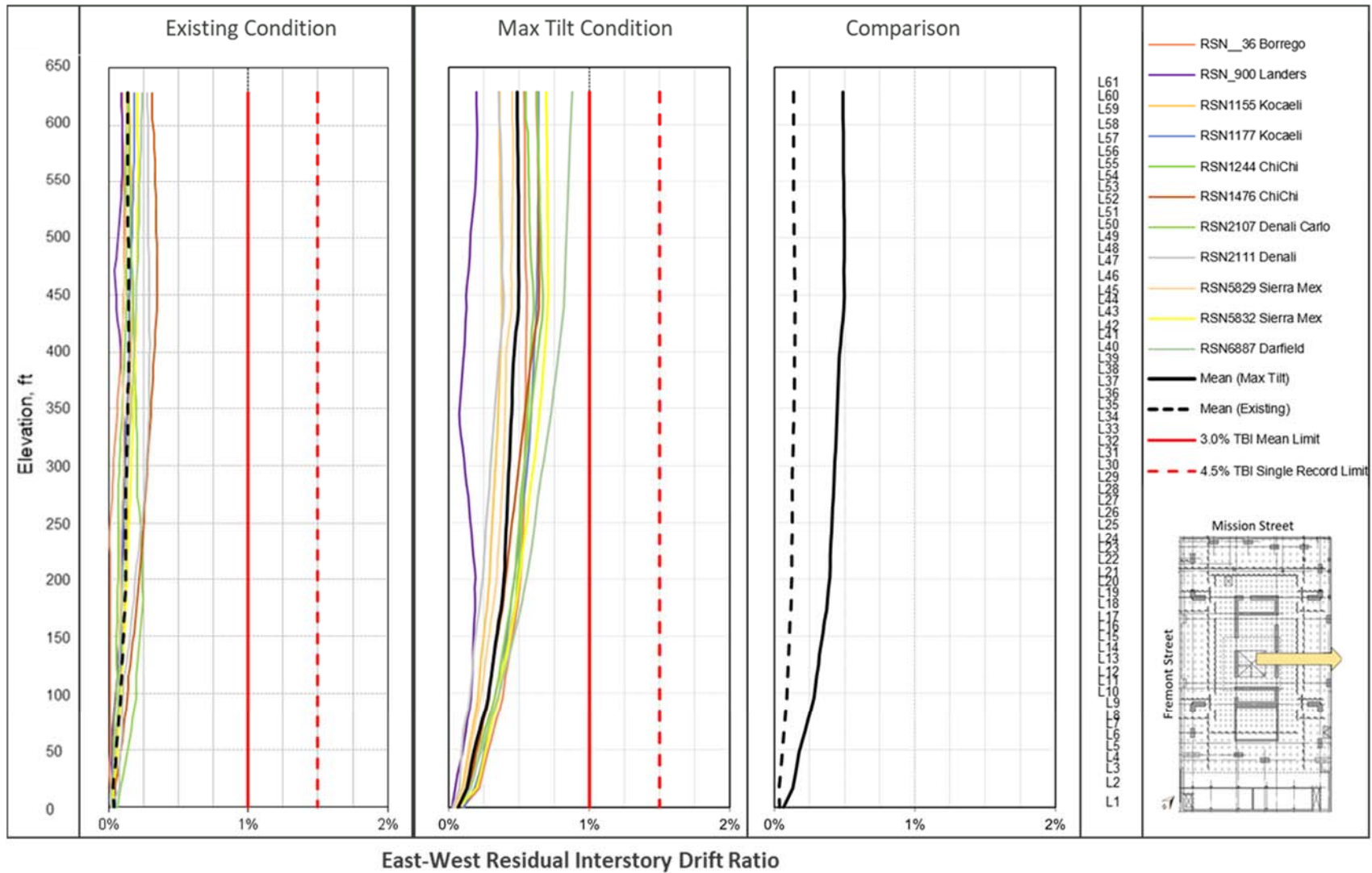
2.5.9 East-West Direction Interstory Drift Ratios



2.5.10 North-South Direction Seismic Residual Interstory Drift Ratios



2.5.11 East-West Direction Seismic Residual Interstory Drift Ratios



2.6